REDUCTION OF SLIDER HEAD VIBRATION DUE TO WINDAGE EXCITATION

BORIPAT NAKNUAL

A THESIS SUBMITTED IN PARTIAL FULFILLMENT
OF THE REQUIREMENT FOR THE DEGREE OF MASTER OF ENGINEERING IN DATA STORAGE TECHNOLOGY

FACULTY OF INTERNATIONAL COLLEGE

KING MONGKUT'S INSTITUTE OF TECHNOLOGY LADKRABANG

2016

KMITL-2016-IC-M-005-006

หัวข้อวิทยานิพนธ์	การลดการสั่นสะเทือนของหัวอ่านจากการกระตุ้นโดยการไหลวนของอากาศ
นักศึกษา	นายบริพัชร นาคนวล
รหัสประจำตัว	54600708
ปริญญา	วิศวกรรมศาสตรมหาบัณฑิต
สาขาวิชา	เทคโนโลยีการบันทึกข้อมูล
พ.ศ.	2559
อาจารย์ที่ปรึกษาวิทยานิพนธ์	ผศ.ดร.มนต์ศักดิ์ พิมสาร

บทคัดย่อ

การสั่นสะเทือนเป็นปรากฏการณ์ที่เกิดอยู่เสมอในธรรมชาติ หนึ่งในนั้นคือการสั่นสะเทือนที่เกิดจากการไหลของอากาศภายในฮาร์ดดิสไดร์ ชิ้นส่วนฮาร์ดดิสไดร์โดยเฉพาะแขนของหัวอ่านและสายสัญญาณของซัสเปนชั่น นั้นไวต่อการสั่นสะเทือนที่ถูกกระตุ้นโดยการไหลวนของอากาศซึ่งอาจเป็นเหตุให้หัวอ่านหาข้อมูลผิดตำแหน่งได้ วิทยานิพนธ์เล่มนี้ได้ทำการทดลองและ ศึกษาเชิงตัวเลขของชุดประกอบหัวอ่าน-เขียน และสายสัญญาณของซัสเปนชั่น ในเบื้องต้นคุณลักษณะการสั่นสะเทือนของชุดประกอบหัวอ่านเขียนและสายสัญญาณของซัสเปนชั่นซึ่งประกอบด้วยความถี่ธรรมชาติและโหมดการสั่นสะเทือนที่ตรงกับความถี่ธรรมชาติจะถูกศึกษาด้วยวิธีเชิงตัวเลขด้วยระเบียบวิธีทางไฟไนท์เอลิเมนต์ หลังจากนั้นผลจากวิธีเชิงตัวเลขจะถูกนำมาเปรียบเทียบกับการทดลองที่วัดได้จากเครื่องเลเซอร์ดอปเพลอร์ไวโบรมิเตอร์ และเครื่องสแกนเลเซอร์ดอปเพลอร์ไวโบรมิเตอร์ ผลการเปรียบเทียบแสดงให้เห็นว่าผลลัพธ์จากสองวิธีนี้ให้ผลลัพธ์ไปในทางเดียวกันในส่วนของการทำนายโหมดการสั่นสะเทือน แต่ความถี่ธรรมชาติมีความแตกต่างมากที่สุด 19.1 เปอร์เซนต์

หลังจากนั้นผลลัพธ์การทดลองและการจำลองแสดงให้เห็นว่าสาเหตุหลักที่ทำให้หัวอ่านสั่นสะเทือนมาจากการไหลวนของอากาศกระตุ้นให้เกิดการสั่นสะเทือนของหัวอ่าน และมีความถี่ 7.6 กิโลเฮิรตซ์

นอกจากนั้นในวิทยานิพนธ์นี้ได้ทำการศึกษาด้วยวิธีการทดลองและเปรียบเทียบผลการสั่นสะเทือนของหัวอ่าน 3 กรณีดังนี้ การติดกาวสายสัญญาณซัสเปนชั่นกับแขนหัวอ่านเขียน (tail tacking) การใช้แฟลบเปอร์ยึดสายสัญญาณซัสเปนชั่น (flapper attachment) และการย้ายตำแหน่งสายสัญญาณของซัสเปนชั่น จากผลการทดลองพบว่าการลดการสั่นสะเทือนของหัวอ่านลดลง 39.3, 10.7 และ 35.7 เปอร์เซนต์ ตามลำดับ วิธีการติดกาวลดการสั่นสะเทือนของหัวอ่านได้ดีกว่าวิธีอื่น ๆ แต่วิธีการนี้ไม่เหมาะในการใช้งานจริง เพราะการ

ติดกาวเพื่อเชื่อมสายสัญญาณของซัสเปนชั่น กับแขนของหัวอ่านนั้น โดยทั่วไปจะเกิดการกระจายตัวของก๊าซ ซึ่งก่อให้เกิดปัญหาการปนเปื้อนของอนุภาคเล็ก ดังนั้นวิธีการย้ายตำแหน่งสายสัญญาณของซัสเปนชั่น จึงถูกแนะนำให้นำไปใช้ในทางปฏิบัติ

Thesis Title: Reduction of Slider Head Vibration Due to Windage Excitation

Student: Boripat Naknual

Student ID: 54600708

Degree: Master of Engineering

Program: Data Storage Technology

Year: 2016

Thesis Advisor: Asst.Prof.Dr.Monsak Pimsarn

ABSTRACT

Vibration is a phenomenon that frequently occurs in nature. One of the examples is flow induced vibration inside hard disk drive (HDD). The mechanical components inside hard disk drive, especially, the actuator arm and flex of suspension (FOS), are very sensitive to flow induced vibration circumstances that may cause recording heads to mis-register, positioning error. Therefore, this thesis aims to experimentally and numerically study vibration characteristics of the head stack assembly (HSA) with FOS. At first, the vibration characteristics of HSA with FOS, namely, natural frequency and corresponding mode shape, were numerically studied using finite element method (FEM). Later, the numerical results were compared with the experimental results, measured using a Laser Doppler Vibrometer (LDV) and Scanning Laser Doppler Vibrometer (SLDV). The comparison reveals that the results obtained from both methods are in good agreement, in term of predicting the mode shape, but the maximum discrepancy of natural frequency is about 19.1%

Later, the experiment and simulation were carried out to investigate the exciting frequency that is the main cause of slider head vibration. The results from both methods reveal that the cause of vibration is mainly due to vortex shedding on FOS and its exciting frequency is about 7.6 kHz.

Moreover, in this thesis, the three methods, namely, tail tacking, flapper attachment and FOS relocation, were experimentally studied to compare their effect on the slider head

vibration. From the experimental results, it was found that the percentage reductions of slider head vibration are 39.3%, 10.7% and 35.7%, respectively. The tail tacking method reduced slider head vibration more than other methods, but this method was not actually utilized in practice. Because this method requires the application of adhesive to bond FOS with the actuator arm and using the adhesive, in general, will create out gassing and leads to particle contamination problem. Therefore, the FOS relocation method is highly recommended in practice.

ACKNOWLEDGEMENT

This thesis would not have been possible without the guidance and the support of several persons who contributed and extended their appreciated assistance in the completion of this research.

First, I would like to sincerely thank The College of Data Storage Innovation King Mongkut's Institute of Technology Ladkrabang for an importance knowledge and information.

I would like to thank Seagate Technology (Thailand) for their equipment and financial supports.

I am utmost gratitude to my advisor Asst.Prof.Dr.Monsak Pimsarn, who has given me valuable suggestions, useful advices to go over all the obstacles in the completion this research.

Finally, I am really grateful to my family for all love, caring and understanding throughout my life.

Boripat Naknual

CONTENTS

CONTENTS (Cont.)

CONTENTS (Cont.)

ABBREVIATION AND SYMBOLS

Abbreviation and Symbols	Definition
ACA	Arm Coil Assembly
DSA	Dynamic Signal Analyzer
FOS	Flex of Suspension
HDD	Hard Disk Drive
HSA	Head Stack Assembly
LB	Load beam
LDV	Laser Doppler Vibrometer
TGA	Tail Gimbal Assembly
VCM	Voice Coil Magnet
A	The surface area of the control volume element
$[C]$	The damping matrix
D	Diameter
F	The vector of fluxes
F_{max}	Force amplitude
$[F]$	The force vector
f	Imposed frequency (cycles/time)
f_i	Natural frequency (cycles per unit time)
f_s	Shedding frequency
i	Square root of -1
$[K]$	The stiffness matrix
L	A characteristic linear dimension
$[M]$	The mass matrix
Q	The vector of conserved variables
Re	Reynolds number
S	Strouhal number
t	Time

ABBREVIATION AND SYMBOLS (Cont.)

Abbreviation and Symbols	Definition
U	Inflow speed
μ	The dynamic viscosity of the fluid
V	The maximum velocity of the object relative to the fluid
Ve	The volume of the control volume element
Ω	Imposed circular frequency (radians/time) = $2\pi f$
Φ	Displacement phase shift (radians)
ν	The kinematic viscosity
ψ	Force phase shift (radians)
ω_i	Natural circular frequency (radians per unit time)
ρ	The density of the fluid

LIST OF FIGURES

LIST OF FIGURES (Cont.)

Figures

LIST OF TABLES

CHAPTER 1

INTRODUCTION

1.1 Backgrounds

Hard disk drive (HDD) areal density growth trends are 10% increase annually. The HDD areal density growth is in paralleled with magnetic size decrease on recording media. Reducing magnetic size requires high precise position control to access the right data. Head Stack Assembly (HSA) is an important component in HDD that a slider is mounted on. HSA can be vibrated while HDD is in operation. This vibration is actually excited by windage excitation.

Windage vibration phenomenon is normally, induced by vortex shedding of air steam. HDD, the windage generated by disk rotation. This is the main source of vibration inside a HDD and it definitely effects on the slider head vibration which may cause the slider positioning error or track miss-registration.

This thesis will mainly focus on the effect of FOS natural frequencies and vortex shedding frequency on the reduction of slider head vibration.

1.2 Objectives

1.2.1 Numerically and experimentally, to study vibration characteristics of HSA and FOS, namely, natural frequency and mode shapes.

1.2.2 To identify the main cause of slider vibration while HDD is in operation and its excitation frequency.

1.2.3 To study the effectiveness of the proposed methods, namely, tail tacking, flapper attachment and FOS relocation on slider vibration.

1.3 Scope of work

In this thesis, the scopes of works are as follow.

1.3.1 The HDD use in this study has following specification

- 3.5" nearline product
- 7200 RPM
- This product is used for high capacity server and cloud market.

1.3.2 In the numerical simulation, the FEM commercial softwares, ANSYS Fluent, ANSYS CFX and ANSYS Classic, are used for modal analysis, harmonic analysis and computation for fluid dynamic analysis.

1.3.3 All components used in the analysis are assumed to have the correct dimensions as specified in the drawings and all surfaces are assumed to be smooth and no slip conditions are applied.

1.3.4 In the experiments, the following measuring machines are employed

- Scanning LDV is used for natural frequency and mode shape identification.
- Single point LDV is used for frequency response in horizontal direction.

1.4 Expected Benefits

1.4.1 To understand the resonance frequencies and mode shapes of the HSA assembly with FOS.

1.4.2 To provide an effective method this will be used for a slider head vibration reduction.

14.3 To increase HDD reliability.

CHAPTER 2

LITERATURE REVIEWS

HDD areal density increase was paralleled by decreasing magnetic size on recording media, smaller magnetic size requires better precise position controlling. Vibration is the main source of exciting force to a slider head which leads to recording head position error. To reduce vibration effect, it is very importance identify resonance frequency of HDD component. Many literatures propose different techniques to reduce HSA vibration which cause of recording position error. To identify the frequency source of vibration is the one of another important issue to propose the effective solution to fix the problem. HSA vibration natural frequency can be analyzed using numerical method and actual measurement. Another problem of HSA vibration is from windage excitation, flow-induced vibration, which occurs while the HDD is in operation another excitation frequency is from wind excitation while drive is operating. This vibration exciting frequency is generated from vortex shedding frequency.

Vortex shedding is an oscillating flow that takes place when a fluid such as air or water flows past a bluff (as opposed to streamlined) body at certain velocities, depending on the size and shape of the body. The frequency at which vortex shedding occurs for an infinite cylinder is related to the Strouhal number. The Strouhal number (St) is a dimensionless number describing oscillating flow mechanisms. The parameter is named after Vincenc Strouhal, a Czech physicist who experimented in 1878 with vortex shedding or singing in the wind.[1]

In 1968, Nakaguchi investigated the correlation between the St and various B/D (dimensional ratio) of height and width of rectangular cylinder through aerodynamic drag tests at attack angle 0 degree, and discovered an interesting fact that there exists the discontinuity of the St at the particular value of B/D = 2.8.[2]

In 1974, Otsuki also investigated this correlation through the aerodynamic force measurement test, there is no attack angles given in his study.[3]

In 1981, Atsushi Okajima from Cambridge University did the experiments on the vortex-shedding frequencies of various rectangular cylinders by using a wind tunnel and in a water tank. The results shown the variation of Strouhal number

varies a width-to-height ratio of the cylinders in the range of Reynolds number between 70 and 2×10^4.[4], [5]

Several researchers have investigated the dynamic characteristics of vibration effect to recording head in HDD. Tsuda, N., et.al. (2003) studied aerodynamic vibration mechanism of HDD Arms predicted by unsteady steady numerical simulation, using unsteady numerical simulation confirm that arm with hole case shown larger vortex effect than arm with no hole case.[6]

In 2004 Yoshiyuki Hirono, et.al., also propose to reduce flow induce vibration by using spoiler, they varies length and thickness of the objects. This result shown that the flow rate can be reduced with the spoiler causes FIV is reduced. It is caused by the fact that the FIV reduction becomes almost constant when the spoiler is longer than the actuator arm length.[7]

K. Ng, et.al. (2011) proposed to reduce flow induce vibration (FIV) by using vortex splitters and flow diverters, the result shown 26% – 27% velocity reduction in horizontal direction. [8]

CHAPTER 3

RELATED THEORY

3.1 Hard Disk Drive (HDD) components [9]

A hard disk drive (HDD), is a data storage device used for storing and retrieving digital information using one or more rigid ("hard") rapidly rotating disks (platters) coated with magnetic material. The platters are paired with magnetic heads arranged on a moving actuator arm, which read and write data to the platter surfaces. Data is accessed in a random-access manner, meaning that individual blocks of data can be stored or retrieved in any order rather than sequentially. HDDs retain stored data even when powered off (Non-volatile).

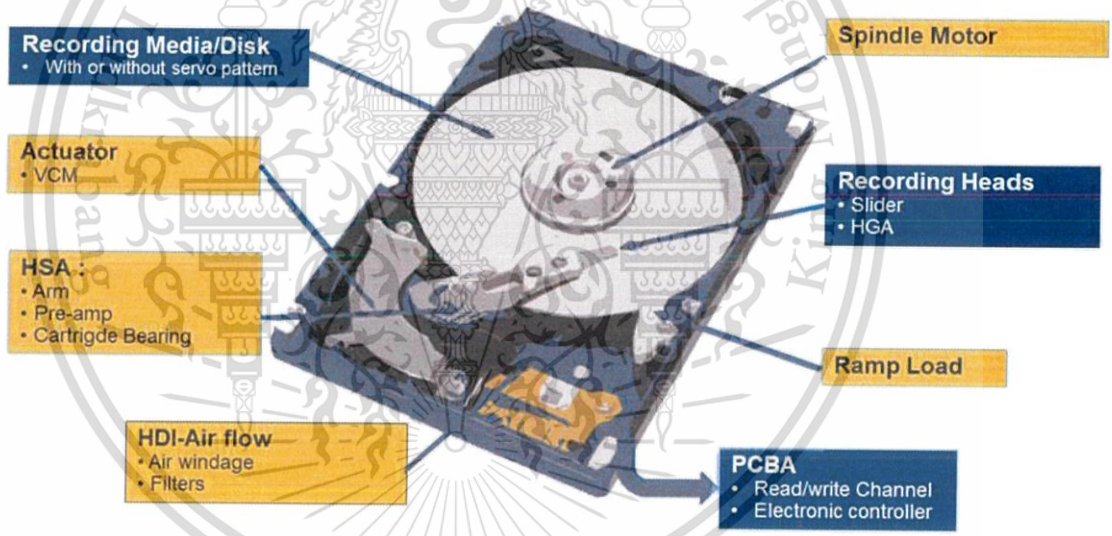

Figure 3.1 Hard disk drive (HDD) components

Head Stack Assembly (HSA) is the actuator arms that position the slider head across the spinning disk. HSA is mounted at the cartridge bearing of the actuator and moved by a permanent magnet and moving coil motor that swings the heads to the desired position.

Head Gimbal Assembly (HGA) is a head-gimbal assembly of a hard disk drive includes a loadbeam (LB) connected to a pivot arm, a slider on which a magnetic head is mounted, an elastic support member having one end coupled to the LB and the other free end portion at which the slider is supported, and a damper provided

between the LB and the slider to attenuate vibration transferred between the LB and the slider. [10]

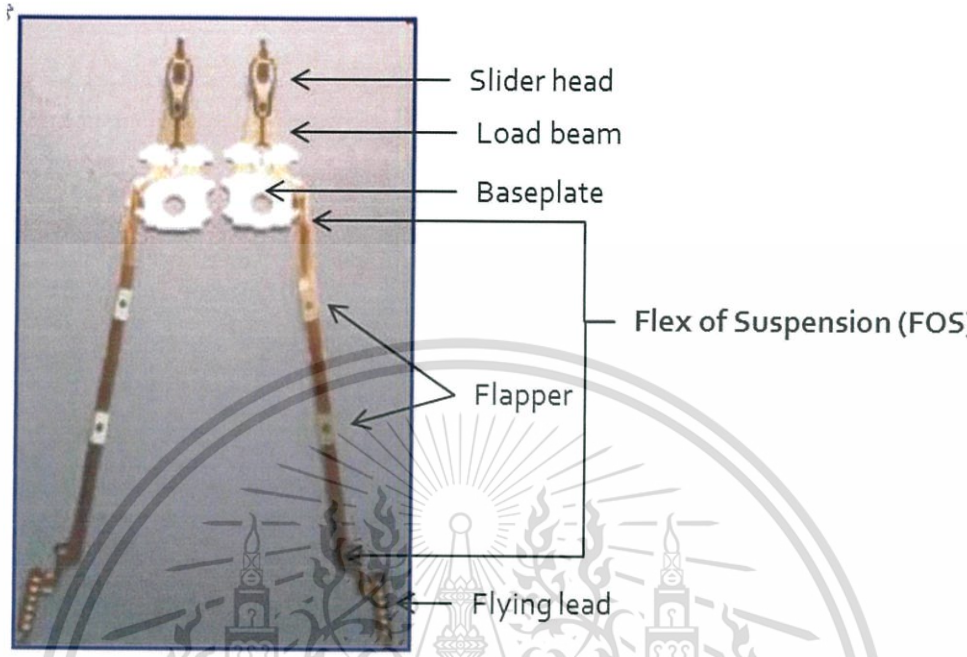

Figure 3.2 Head gimbal assembly (HGA) components

3.2 Flow-induced vibration [11]

Vortex shedding is an oscillating flow that takes place when the air past actuator arm. The air past actuator arm creates low pressure and force on the downstream side of actuator arm. A function of the upstream velocity and the dimension of actuator arm is relate to vortex shedding frequency, f_s, that will excite TGA flex at downstream side. Where, U is upstream velocity, and D is actuator thickness.

3.2.1 Vortex shedding frequency [12]

Vortex shedding is an oscillating flow that takes place when the air past actuator arm. The air past actuator arm creates low pressure and force on the downstream side of actuator arm. A function of the upstream velocity and the dimension of actuator arm is related to vortex shedding frequency, f_s, that will excite TGA flex at downstream side.

$$f_s = \frac{SU}{D} \tag{3.1}$$

Where, U is the upstream velocity, and D is the actuator thickness.

3.2.2 Reynolds number

The Reynolds number is defined as the ratio of momentum forces to viscous forces and consequently quantifies the relative importance of these two types of forces for given flow conditions. Reynolds number is also used to characterize different flow regimes within a similar fluid, such as laminar or turbulent flow. [13]

$$Re = \frac{Inertial\ force}{Viscous\ force} = \frac{\rho VL}{\mu} = \frac{VL}{\nu} \tag{3.2}$$

Where, V is the average velocity of the object relative to the fluid, L is a characteristic linear dimension μ is the dynamic viscosity of the fluid, $\vartheta(nu)$ is the kinematic viscosity ρ is the density of the fluid.

3.3 Finite element analysis

To study hard disk drive vibration phenomenon is very important. Generally the numerical method such as Finite Element Analysis (FEA), can be employed to simulate fluid dynamic and vibration response of hard disk drive.

3.3.1 Computation for fluid dynamics (CFD)

CFD is a branch of fluid mechanics that uses numerical analysis and algorithms to solve and analyze problems that involve fluid flows. Computers are used to perform the calculations required to simulate the interaction of liquids and gases with surfaces defined by boundary conditions.

This thesis uses finite volume method to solve fluid dynamic boundary condition of spinning HDD. In the finite volume method, the governing partial differential equations are recast in a conservative form, and then solved over discrete control volumes. The finite volume equation is in the form of

$$\frac{\partial}{\partial t}\iiint Q\, dV_e + \iint F\, dA = 0 \tag{3.3}$$

Where, Q is the vector of conserved variables F is the vector of fluxes V_e is the volume of the control volume element A is the surface area of the control volume element.

3.3.2 Modal analysis in finite element method

A modal analysis determines the vibration characteristics (natural frequencies and mode shapes) of a structure. The natural frequencies and mode shapes are important parameters in the design of a structure for dynamic loading conditions.

The modal analysis in structural mechanics is to determine the natural mode shapes and corresponding frequencies of an object or structure during free vibration. The finite element method (FEM) is one of the numerical methods used to perform this analysis. The generalized dynamic equation of structure motion is given as

$$[M][\ddot{U}] + [C][\dot{U}] + [K][U] = [F] \tag{3.4}$$

Where, $[M]$ is the mass matrix, $[\ddot{U}]$ is the 2nd time derivative of the displacement $[U]$ (i.e., the acceleration), $[\dot{U}]$ is the velocity, $[C]$ is a damping matrix, $[K]$ is the stiffness matrix, $[F]$ is the force vector.

In modal analysis, the equation of motion is first rebuked to an un-damped system, and expressed in matrix notation as

$$[M]\{\ddot{U}\} + [K]\{U\} = \{0\} \tag{3.5}$$

ANSYS solver will use this matrix equation to solve mode shapes and natural frequencies, the eigenvectors and eigenvalues, respectively.

3.3.3 Harmonic analysis in finite element method

Harmonic analyses are used to determine the steady-state response of a linear structure to loads that vary harmonically with time, and this simulation will help to designs resonance structure with force application.

This analysis technique calculates only the steady-state, forced vibrations of a structure. The transient vibrations, which occur at the beginning of the excitation, are not accounted for in a harmonic analysis. In several, the results obtained from modal analysis are partially extracted and employed in the harmonic analysis, and the governing equation is same as in Eq. (3.4).

In this thesis, the ANSYS software is employed to solve the frequency response function and provide a bode plot for natural frequency analysis.

3.4 Resonance measurement

The frequency response functions are used in vibration and modal testing. The purpose of modal testing is the natural frequencies measurement and mode shapes of a structure. The frequency response function is the ratio of output and input of the vibration model.

Figure 3.3 Frequency response amplitude model

In the measurement, the voltage signal from LDV to measure vibration at slider head to be the output signal. The input signal is from dynamic signal analyzer source generator that excites the HSA.

This gain amplitude will be used to compare the resonance result of propose methods and current method to justify the resonance performance of slider head. Its value can be obtained from Eq. (3.6).

$$|Gain|_{dB} = 20 \log \left| \frac{Output\ Voltage_{Velocity}}{Input\ Voltage_{Velocity}} \right| \quad (3.6)$$

CHAPTER 4

RESEARCH METHODOLOGY

4.1 Introduction

In this thesis, the research methodology will be carried out as follow,

1. Identify the product to study, and the selected product is 3.5" Nearline product that is mainly used for high capacity in server rack and cloud server.
2. Prepare 3D model (Solid modeling) and establish finite element model (FEM) to simulate vibration characteristic of HSA with FOS.
3. Prepare an actual experiment and measure a resonance frequency from actual part using LDV and SLDV.
4. To compare FEM and experimental results.
5. Prepare 2D model to study vortex shedding frequency that is generated by windage.
6. Prepare 3D model for fluid and solid coupling to study resonance frequency that is excited by windage.
7. To compare FEM and actual experimental result.
8. Propose the methods to reduce a slider head vibration.
9. Study resonance frequency and amplitude of 3 methods.
10. Compare the experiment results, to justify the effectiveness of the proposed methods.

4.2 Finite element modeling for modal analysis

4.2.1 Problem Description

The head stack assembly with FOS used in finite element analysis is composed of actuator machining, bearing, coil, glue, bobbin, baseplate, loadbeam, PZT, PZT glue and FOS, as shown in Figure 4.1

Table 4.1 Element type of each component

Component	Element Types
Actuator machining	3D Solid
Pivot Bearing	3D Solid Combin (Spring)
Coil	3D Solid
Glue	3D Solid
Bobbin	3D Solid
Baseplate	3D Solid
Loadbeam	2D Shell
PZT	3D Solid
PZT glue	3D Solid
FOS	3D Solid

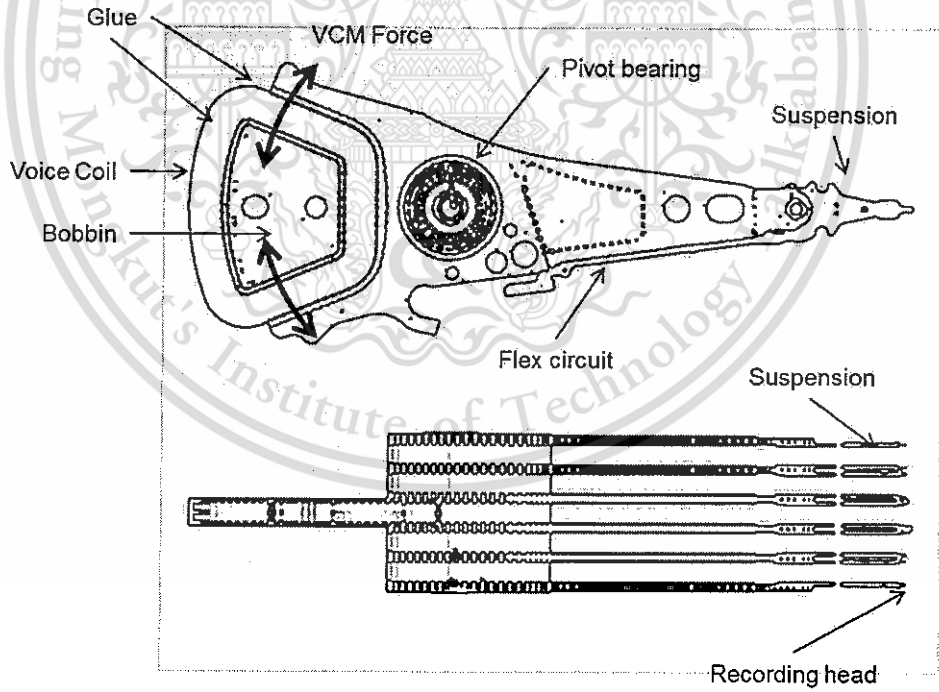

Figure 4.1 Schematic diagram of head stack assembly with FOS

In the modal analysis, the number of natural frequencies and mode shapes that are extracted is two hundreds and the sub-space numerical technique, available in ANSYS is chosen.

In the modal analysis of a HSA, it is fixed to pivot bearing surface, bottom and top. Each HSA components are made of different materials and their properties are specified in Table 4.2.

4.2.2 Material properties

Table 4.2 Material properties for resonance simulation. [14]

Material	Specific properties	Value	Unit
Stainless steel	Elastic modulus	1.9×10^{11}	Pa
	Poisson's ratio	0.305	
	Density	7.791×10^{-6}	kg/mm^3
Aluminum Alloy	Elastic modulus	7.1016×10^{10}	Pa
	Poisson's ratio	0 .33	
	Density	2.7242×10^{-6}	kg/mm^3
Copper	Elastic modulus (EX)	0.23×10^{11}	Pa
	Elastic modulus (EY)	0.04×10^{11}	Pa
	Elastic modulus (EZ)	0.04×10^{11}	Pa
	Poisson's ratio	0.345	
	Density	0.2168×10^{-5}	kg/mm^3
Glue	Elastic modulus	0.21×10^{10}	Pa
	Poisson's ratio	0.35	
	Density	1.5×10^{-6}	kg/mm^3

4.2.3 Boundary condition and contact condition

The HSA is fixed at pivot bearing datum and the top of pivot bearing datum which is fixed by screw clamp. The coil is excited by Voice Coil Motor (VCM) force. TGA tail or flex of suspension is constrained with ACA arm with coupling node technique. Master nodes are defined on the arm at flapper and glue locations and slave nodes are defined on the flex of suspension.

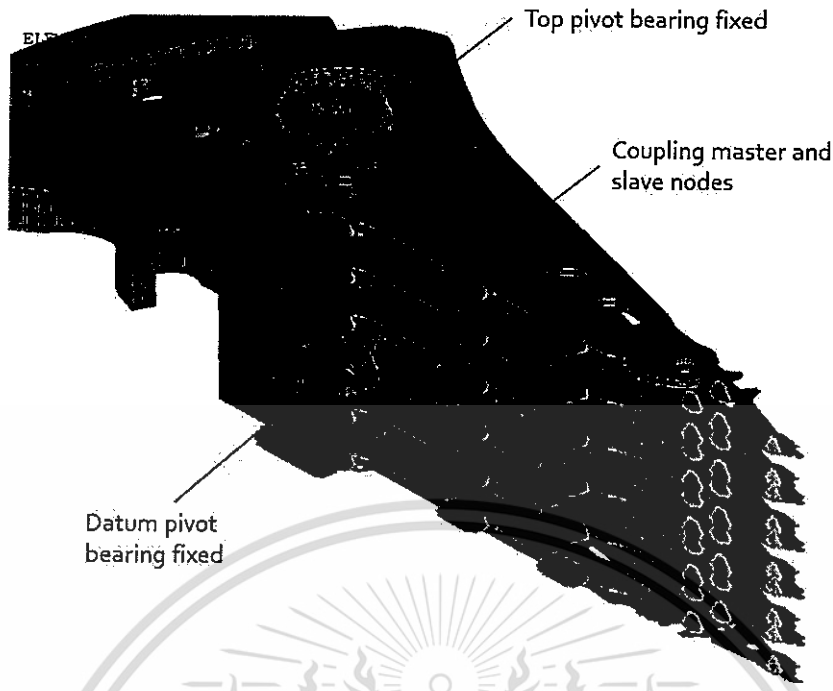

Figure 4.2 Boundary and contact conditions of modal analysis

In this modal simulation, connecting between each component is very importance to provide the precise result. Therefore, in this thesis node bonding technique is employed and can be shown in Figure 4.3. Connection between a bearing inner race and a bearing outer race is a spring element.

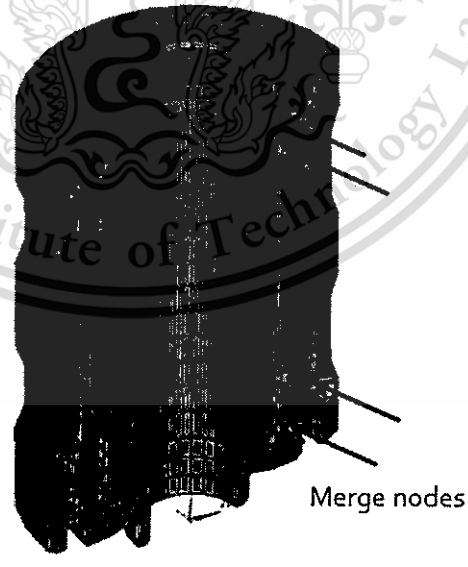

Figure 4.3 Merge nodes between bearing shaft and bearing sleeve

4.3 FEA modeling for harmonic analysis

4.3.1 Fluid dynamics by ANSYS CFX

The HDD is in operation condition, it will generate flow of air stream inside the HDD. This air flow will excite the HSA and create a slider vibration. Slider vibration simulation requires function of the excitation force. ANSYS CFX will provide the pressures inside the HDD on each location, and it can be transferred to forces and applied to FEM harmonic analysis model.

4.3.2 Fluid and solid coupling technique

There are many techniques to combine fluid and solid simulation. In this thesis, the manual transfer of the excitation force from a fluid dynamic analysis is used. The coupling step will be carried out as follows,

1. Prepare the FEA model for fluid dynamic analysis using ANSYS CFX to simulate HDD which is in operating condition. This simulation will provide air velocity and air pressure inside the HDD on all nodes.
2. The pressure will be converted to force using commercial feature in ANSYS CFD post processing.
3. This thesis focuses on the windage excitation force that excites at FOS, therefore the force will be applied on FOS only.

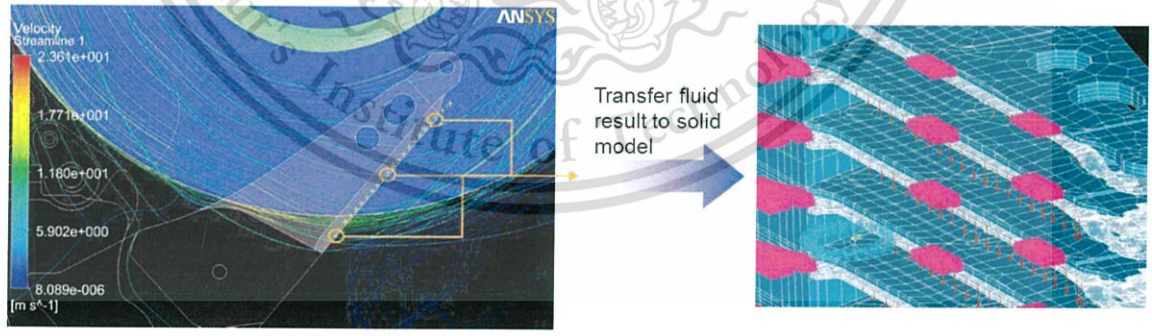

Figure 4.4 Applying force from fluid dynamic analysis to harmonic analysis

4.3.3 Harmonic analysis

Harmonic analysis is the vibration simulation that requires a forcing function and combines a damping term in the calculation. This simulation will provide frequency response function according to Figure 5.9.

To combine fluid dynamics analysis with harmonic analysis by getting the excitation force from fluid dynamic result and apply fluid dynamic force into harmonic analysis. The result from harmonic analysis provides Frequency Response Function (FRF) of the HSA for observing the vibration frequency from wind excitation that is related to slider head vibration.

4.4 FEA modeling for CFD to study vortex shedding frequency

4.4.1 Problem description

In HDD, as disks are spinning and the actuator arms are rotating. The air velocity will create vortex shedding frequency at the actuator arm tailing edge. Therefore, in this thesis, vortex shedding frequency, related to head vibration, is numerically studied. The vortex shedding frequency simulation is assumed to be 2D problem and the ANSYS Fluent is utilized.

The finite element model is created from hard disk drive cross section according to picture in Figure 4.5. The model scope is identified to calculate only 2 arms and 1 disk surface. The simplified model represents inner and outer arms which normally provide the difference result when compared it with the actual measurement.

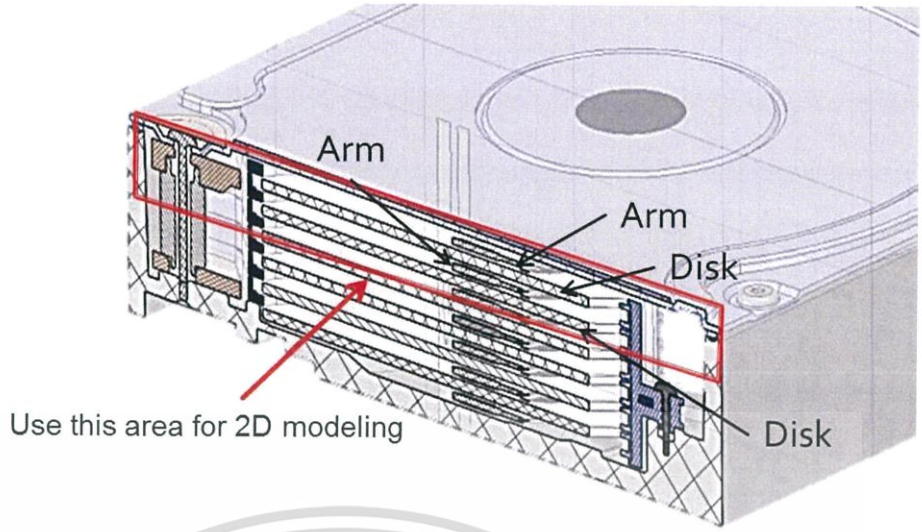

Figure 4.5 2D finite element model of HDD cross section used in ANSYS Fluent

4.4.2 Material properties for fluid dynamic analysis

The fluid properties use in fluid dynamic analysis in hard disk drive simulation is as follow,

1) Fluid is air
2) Ambient temperature is 25 °C,
3) Air density is 1.225 kg/m^3
4) Air viscosity is 1.7894×10^{-5} kg/m-s

4.4.3 Meshing

In order to capture the boundary layer, thin film mesh at wall surface using inflation 10 layers with 0.272 transition ratio and 1.2 growth rate is employed. The 5×10^{-2} mm element size is applied to actuator arm edge and the 0.1 mm element size is applied to the rest surface.

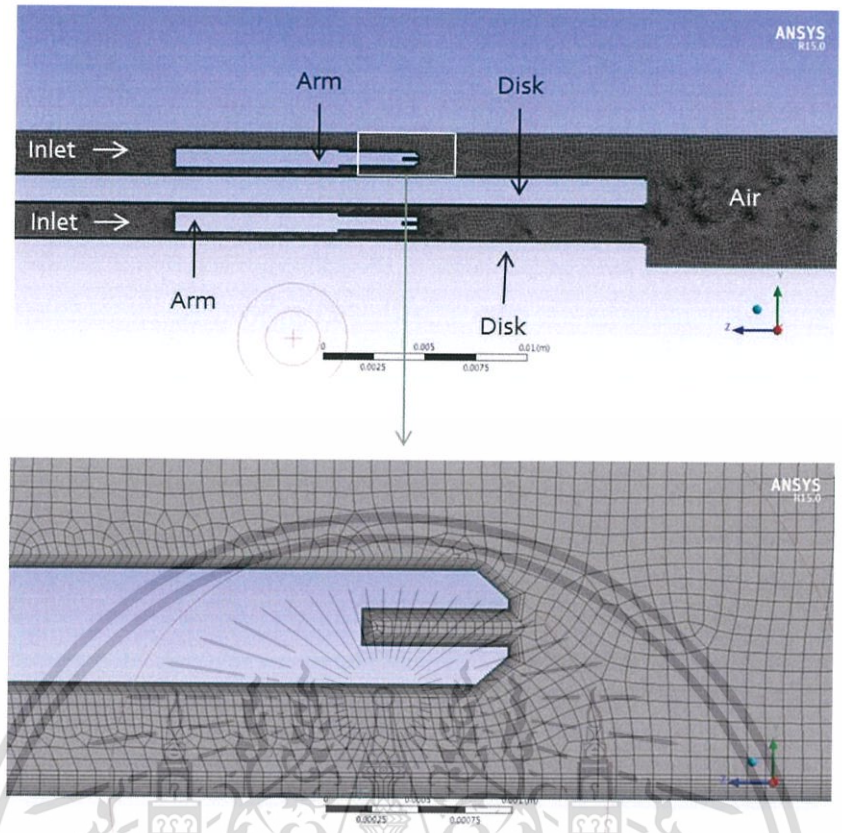

Figure 4.6 2D finite element model meshing

Inflation layers are critical component of CFD mesh. The wall condition will result in that the velocity decreases non-linearly up to a point where the fluid will have zero velocity at the wall. This is what is termed the "no slip" wall condition in CFD. This will provide more accurate resolution of the boundary layer. For certain simulations, such as, flows with strong wall-bounded effects, this resolution is absolutely necessary.

4.4.4 Boundary Condition

This model is analyzed in transient analysis, laminar viscous model, applied inlet velocity at 25 m/s, a stationary wall with no slip option for all surfaces, and outlet pressure is 1 atm.

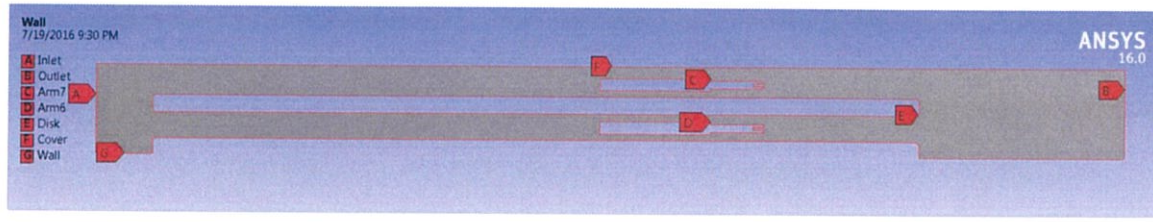

Figure 4.7 2D Boundary condition of fluid dynamic analysis

4.5 Actual measurement

4.5.1 Experiment setup

The experiments were carried out using Scanning LDV system at Seagate Technology (Thailand) Ltd, shown in Figure 4.8. Hard disk drive spins at 7200 RPM. Actuator arm was located at inner, middle and outer zone of disk. To measure the vibration caused by wind-induced vibration, the test model was setup to measure response frequency range 500 – 15,000 Hz which are related to Head Stack Assembly (HSA). TGA vibration was measured by Laser Doppler Vibrometer (LDV) at resolution line 1600. LDV was setup 125 m/s/V, low pass filter at 100 kHz and high pass filter at 100 Hz.

There are 2 types of resonance measurement in this experiment; one is the LDV measurement at slider to predict recording head mis-position. Another one is Scanning LDV measurement to measure actuator arm and flex resonance especially.

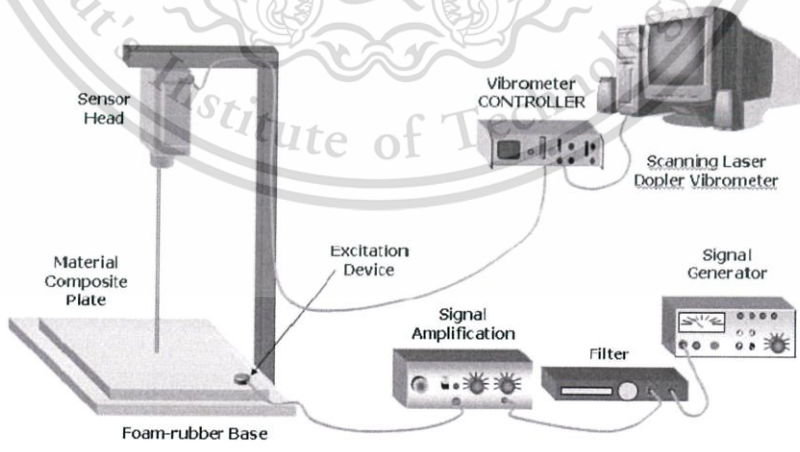

Figure 4.8 Schematic of windage excitation power spectrum test

The equipment's used in the experiment

1. Dynamic Signal Analyzer (DSA)
2. Laser Doppler Vibrometer (LDV)
3. Power Supply (5/12 Volts PC power supply)

Table 4.3 LDV setup

Tracking	FAST
Velocity	125 mm/s/V
Lowpass Filter	100 kHz
HighPass Filter	100 Hz

4.5.2 FRF actual measurement of a slider

A Bode plot is a graph of the magnitude (in dB) or phase of the transfer function versus frequency. The gain is plotted from output magnitude divided by input magnitude in log scale. The HSA is setup in drive while drive is spinning. The HSA is excited by a function generator or a source generator from a dynamic signal analyzer at the HSA VCM coil. A LDV laser beam is placed on a slider at horizontal direction to measure slider vibration. The result of LDV measurement setup is shown in figure 5.9.

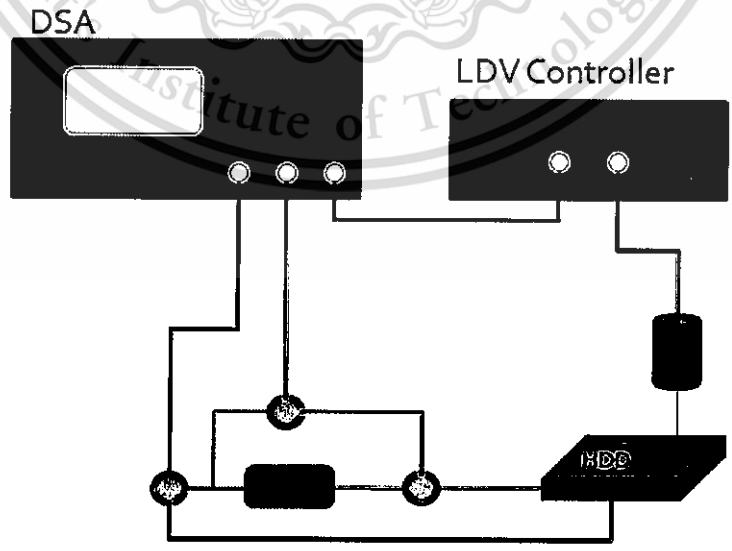

Figure 4.9 Schematic of VCM excitation bode test setup

DSA setup for VCM excitation bode test

Setup applies only to HP35670A. Channel 1 (Ch1) is connected to the 1 ohm resistor terminals for voltage drop measurement. Channel 2 (Ch2) is connected to the velocity output of LDV. Test determines frequency response, defined as Ch2/Ch1. The source signal from the DSA is connected to the VCC of the actuator.

Cable Connection for VCM Excitation Bode Test

1. Connect the LDV Controller velocity output to channel 2 of DSA using a BNC cable.
2. Connect the source of DSA in series through the 1 ohm resistor to the HSA coil using a BNC cable.
3. Measure voltage drop across the 1 ohm resistor by connecting channel 1 to the resistor terminals using a BNC cable in Figure 4.9.

Table 4.4 VCM excitation bode display setup

Disp Format	UPPER/LOWER
Measure Data	CHANNEL 1 FREQ RESP 2/1 or DJOM(FREQ RESP 2/1) CHANNEL 2 FREQ RESP 2/1 or DJOM(FREQ RESP 2/1)
Active Trace	A
Trace Coord	dB MAGNITUDE
Scale	AUTOSCALE ON
Active Trace	B
Trace Coord	PHASE
Scale:	AUTOSCALE ON

Table 4.5 VCM excitation bode test setup

Inst Mode	SWEPT SINE
Freq	START Refer to Product Specific HSA VCM Response Specification STOP Refer to Product Specific HSA VCM Response Specification SWEEP LOG

	SWEEP UP SWEEP AUTO RESOLUTION 450 POINT/SWEEP
Input	CHANNEL 1 AUTO RANGE XDCR UNITCH 1 SETUP XDCR UNIT OFF CHANNEL 2 XDCR UNITCH 2 SETUP XDCR UNIT ON XDCR UNIT 1 V/EU XDCR UNIT LABEL m/s
Source	LEVEL 1 Vpk
Avg	SETTLE TIME 40 Cycles INTEGRATE TIME 40 Cycles

4.5.3 Windage actual measurement at slider setup

A windage is the wind excitation model that applied the excitation force from fluid dynamics analysis. This thesis applied force on the FOF only. It will confirm the related frequency between windage force and slider vibration.

A windage plot is a graph of the magnitude (in velocity or displacement) or versus frequency. Windage is power spectrum of vibration measurement in time domain. The HSA is setup in drive while drive is spinning. HSA is excited wind that generated from spinning disk. LDV is placed on slider at Y direction to measure slider off track vibration. This measurement is representing actual working function of HSA in drive.

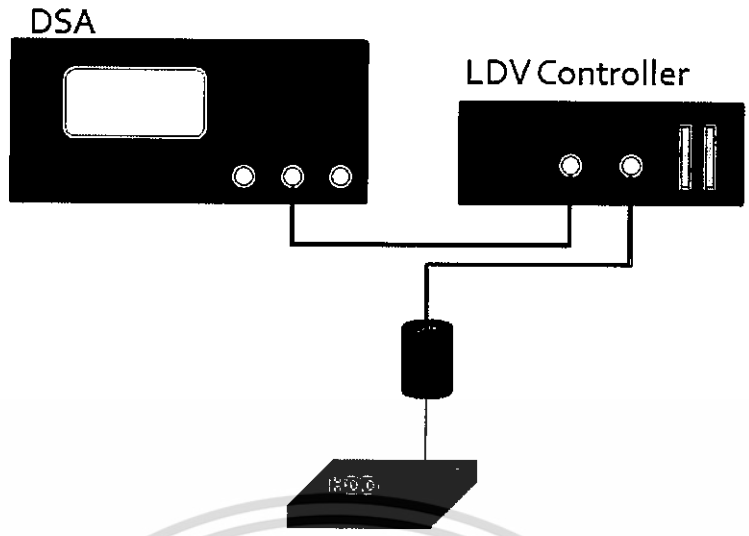

Figure 4.10 Schematic of windage excitation power spectrum test setup

DSA setup for windage excitation power spectrum test

Setup applies only to HP35670A. Channel 1 is connected to the velocity output of LDV. Test determines power spectrum of channel 1.

Mechanical setup

1. Install a HSA into a modified HDA base deck.
2. Attach spin-up PCB Card to the HDA base and power-up the spin-up card.
3. Manual move the HSA to an outer diameter (OD) location. Secure the HSA location by placing tape between the HSA and the bottom of the deck.
4. Put the modified HDA on the periscope fixture. Adjust the z-level of the modified HDA to ensure that the mirror is on the same level as the slider to be measured.

Cable connection for windage excitation power spectrum test

1. Connect the LDV controller velocity output to channel 1 of DSA using a BNC cable in Figure 4.10.

Table 4.6 Windage display setup

Disp Format	Single
Meas Data	CHANNEL 1, PWR SPEC CHANNEL 1

Active Trace	A
Trace Coord	LINEAR MAGNITUDE
X-axis	LINEAR
Scale	AUTOSCALE ON

Table 4.7 Windage measurement setup

Inst Mode	FFT ANALYSIS
Freq	START Refer to Product Specific HSA Windage Response Specification STOP Refer to Product Specific HSA Windage Response Specification
Resolution line	1600
Window	HANNING
Input:	CHANNEL 1 CH1 Auto FRONT END CH1 SETUP INPUT LOW: FLOAT COUPLING: AC ANTITIALIAS: ON A WT FLTR: OFF ICP SUPLY: OFF XDCR UNIT CHANNEL1 SETUP CHANNEL 1 XDCR UNIT OFF
Source	OFF
Trigger	CHANNEL 1 TRIGGER SETUP: FREE RUN TRIGGER
Avg	ON NUMBER AVERAGES: 60 FAST AVG: OFF REPEAT: OFF OVLD REJ: OFF

4.5.4 Scanning LDV setup

Scanning Laser Doppler Vibrometer (SLDV) is an instrument for rapid non-contact measurement and imaging of vibration. The operating principle is based on the Doppler Effect, which occurs when light is back-scattered from a vibrating surface. Both velocity and displacement can be determined by analyzing the optical signals in different ways. A scanning laser vibrometer integrates computer-controlled X and Y scanning mirrors and a video camera inside an optical head. The laser is scanned point-by-point over the test object's surface to provide a large number of very high spatial resolution measurements. This sequentially measured vibration data can be used to calculate and visualize animated deflection shapes in the relevant frequency bands from frequency domain analysis.

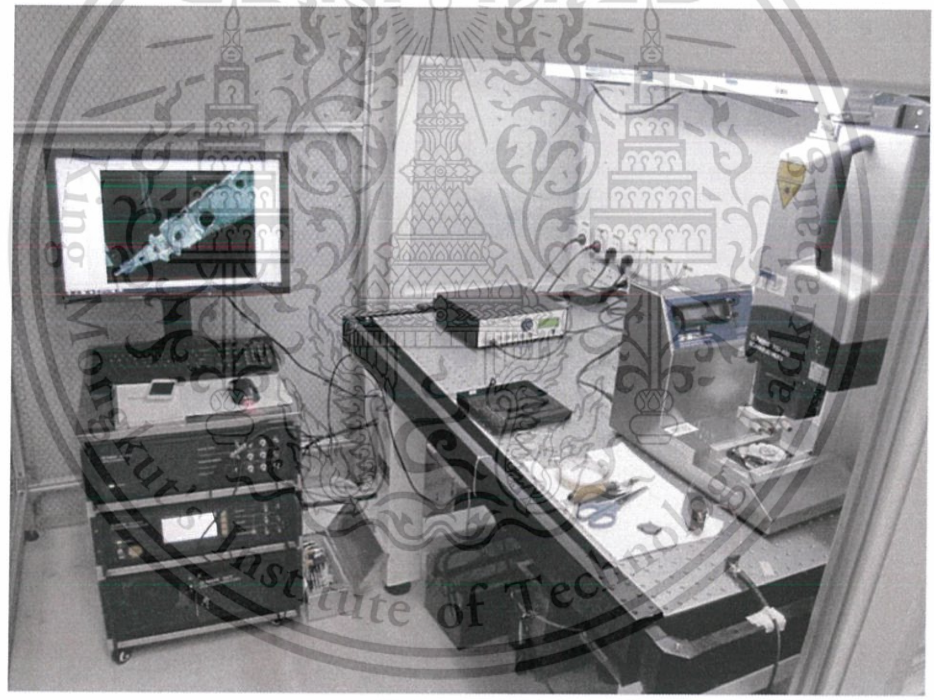

Figure 4.11 Scanning Laser Doppler Vibrometer systems

Scanning LDV equipment

1. Junction box generator and analysis the dynamic signal.
2. Vibrometer controller, Receive the LDV vibration signal.
3. PC, run the Scanning LDV software.
4. Light, provide the light.

5. Monitor, observe the Scanning head image and operate the scanning LDV software.
6. Scanning Head, the major of the scanning LDV equipment, can generate the laser.
7. Spin box, spin the drive motor.

Scanning LDV is capable to scan multi points and pronounce all points result in 1 graph so scanning point on actuator arm and HSA flex of suspension have to be identify in Figure 4.12. Testing boundary and resolution is defined using Scanning LDV software. The number of scanning points has to be good enough to capture resonance behavior of head stack assembly.

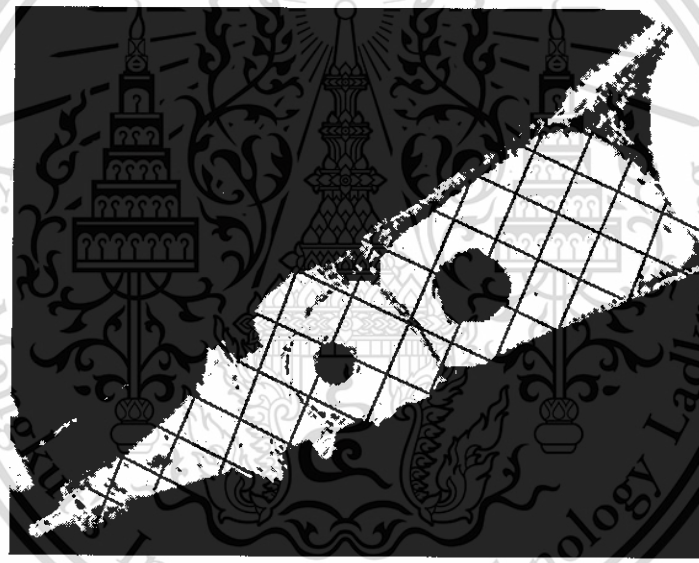

Figure 4.12 Identify scanning point on actuator arm and HSA FOS

4.6 Proposed vibration reduction methods

From the finite element studies and actual measurement result, it was found that, the slider resonance frequency is around 7.6 kHz and related to the FOS vibration which is excited by windage when drive is in operation. In this thesis, the method proposed to reduce the slider vibration as follow,

1. Apply glue to add the damping into the system, namely, tail tacking.

2. Increase stiffness of the FOS by changing flapper attached location, expect to change the natural frequency of the FOS by putting constrain into the system. This method is called flapper attachment.
3. Reduce force excitation for the windage by relocating the FOS into the arm slot. This method is called. FOS relocation.

4.6.1 Tail tacking

This method is proposed to apply glue into HSA system to add more damping to the system. Figure 4.13 shows the locations where the glue dots are applied to.

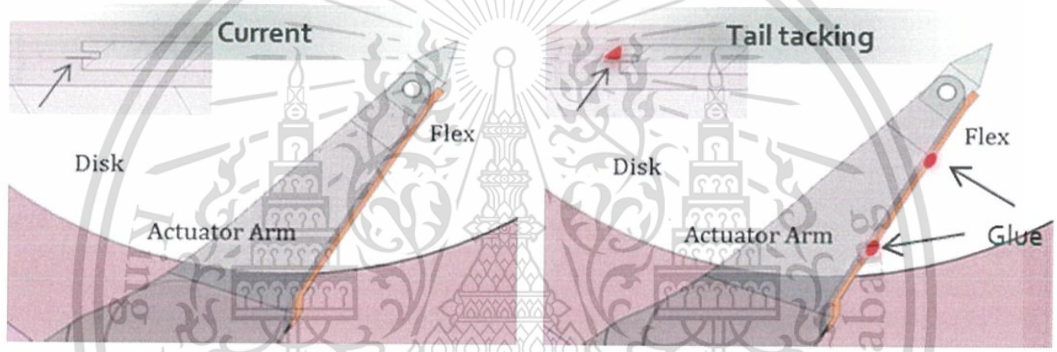

Figure 4.13 Current arms versus tail tacking

4.6.2 Flapper attachment

The objective of this solution is designed to minimize HSA FOS vibration and develop the new solution to eliminate glue tacking. Flappers are stainless layer on HGA FOS; they will be folded before loaded HGA FOS in to actuator arm groove. Flappers are shown in Figure 4.14.

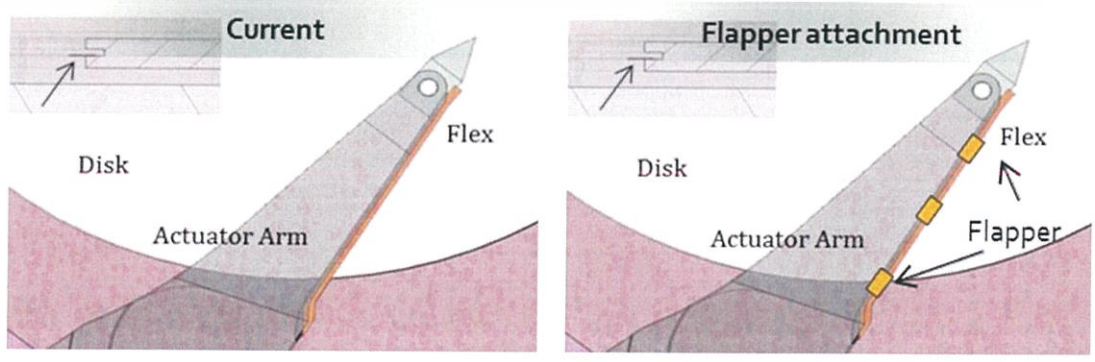

Figure 4.14 Current arms versus flapper attachment

This technique will fix the FOS to the arm groove to increase FOS stiffness and reduce the vibration effect to slider. The flapper attachment points are varied to find the best location of flapper attachment.

4.6.3 FOS relocation

In this method, the FOS placement position is moved inside the actuator arm. This method is so-called FOS relocation. With this technique, it is expected that the vortex shedding source will be moved for away from the FOS. Therefore, the FOS vibration amplitude can be reduced and also it leads to less vibration to a slider head.

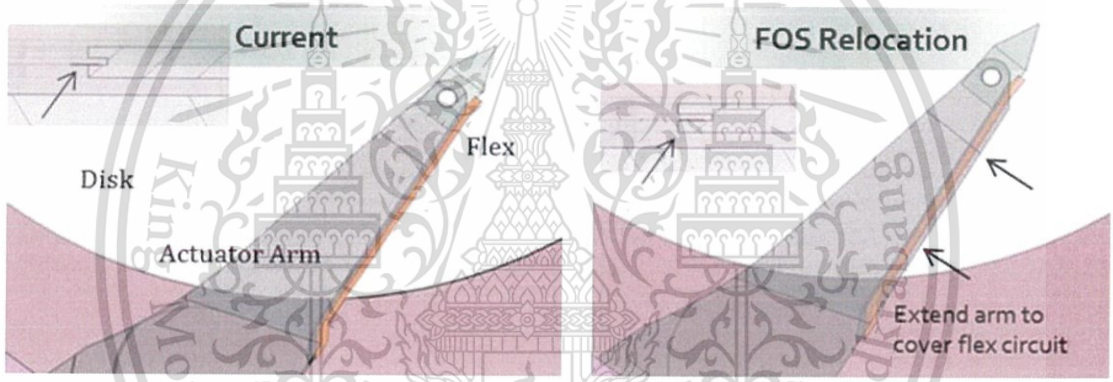

Figure 4.15 Current arms versus FOS relocation

CHAPTER 5

EXPERIMENTAL RESULT AND DISCUSSION

5.1 Modal analysis result

In this thesis, the interested mode shapes that were chosen to study are in the frequency range of 0 to 30 kHz. The mode shapes are shown in Figure 5.1 to Figure 5.8. The HSA and FOS mode shapes will be plotted and described below.

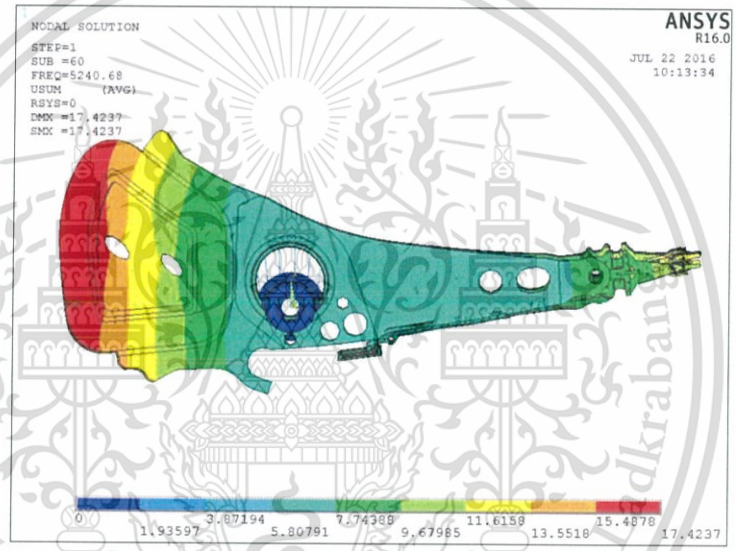

Figure 5.1 First system mode, 5240 Hz

Figure 5.1 shows the first HSA system mode or the rigid body mode. Its associated natural frequency is 5.2 kHz. This mode tends to create this slider positioning error or track-misregistration.

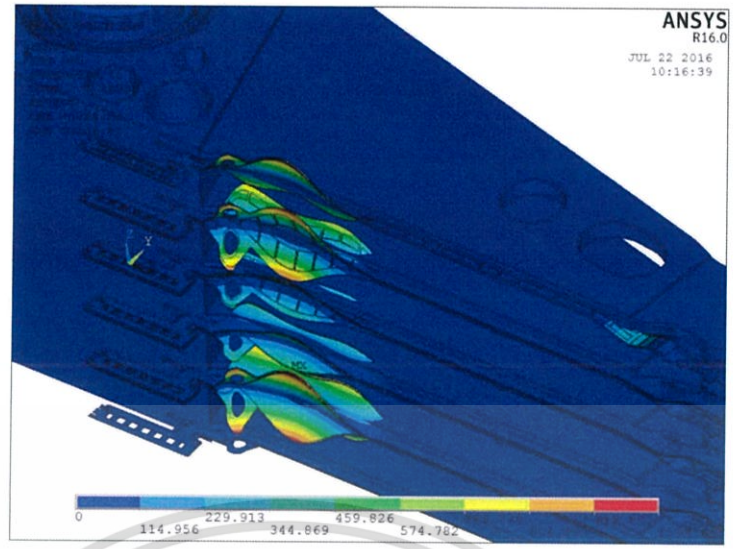

Figure 5.2 FOS first bending at rear side, 6328 Hz

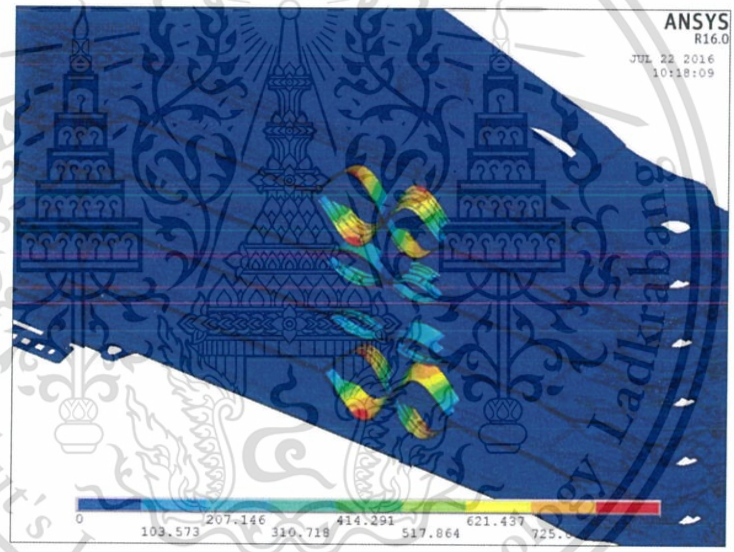

Figure 5.3 FOS second bending at middle side, 6658 Hz

Figure 5.2 display the first FOS bending mode shape at 6.328 kHz. This mode shape is similar to the first bending mode shape of a simply support beam.

Figure 5.3 shows the second FOS bending mode shape at 6.658 kHz. The mode shape is appeared at middle zone of the FOS.

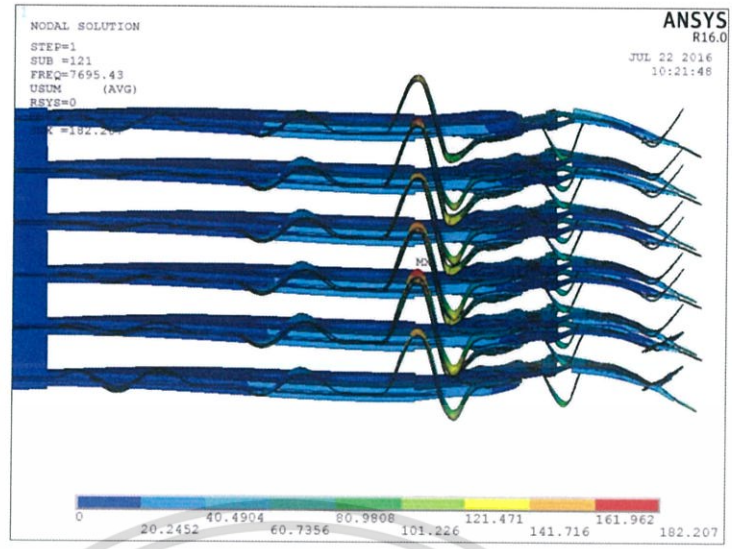

Figure 5.4 Arm first bending and FOS second bending @ front side, 7695 Hz

Figure 5.4 shows the arm first bending and FOS second bending mode. Its associated natural frequency is 7.695 kHz. This mode is coupling of arm bending and the FOS bending mode. The suspension is bended because of arm bending effect.

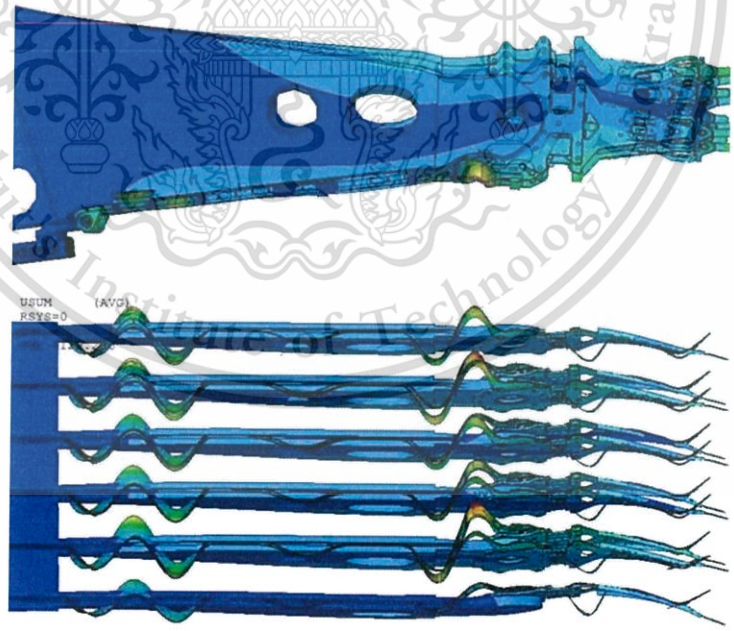

Figure 5.5 Arm first torsion and FOS third bending at front and rear sides, 7963 Hz

Figure 5.5 shows the arm first torsion and FOS third bending mode. Its associated natural frequency is 7.963 kHz. This mode shows coupling frequency between the arms and the FOS. This mode tends to create this slider positioning error or track-misregistration because the suspensions have been twisted in horizontal direction and also caused by arm torsion behavior.

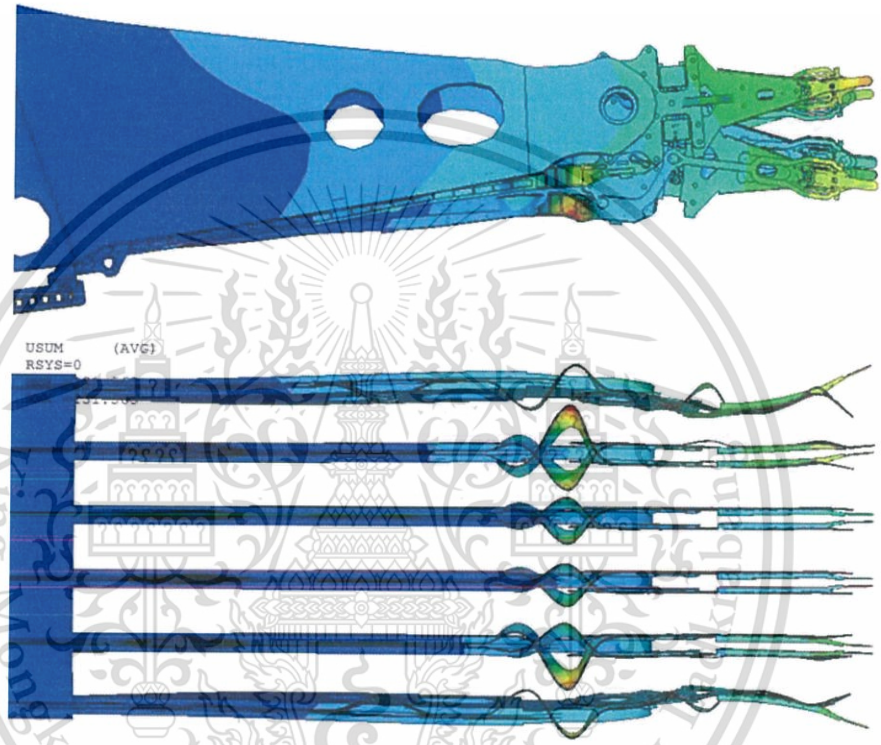

Figure 5.6 Arm first torsion (Scissors) and FOS second bending at front side, 8834 Hz

Figure 5.6 shows the arm first torsion and FOS third bending mode. Its associated natural frequency is 8.834 kHz. The top and bottom arms move in opposite on direction horizontal plane, so this mode is called arm scissor mode. This mode tends to create this slider positioning error or track-misregistration.

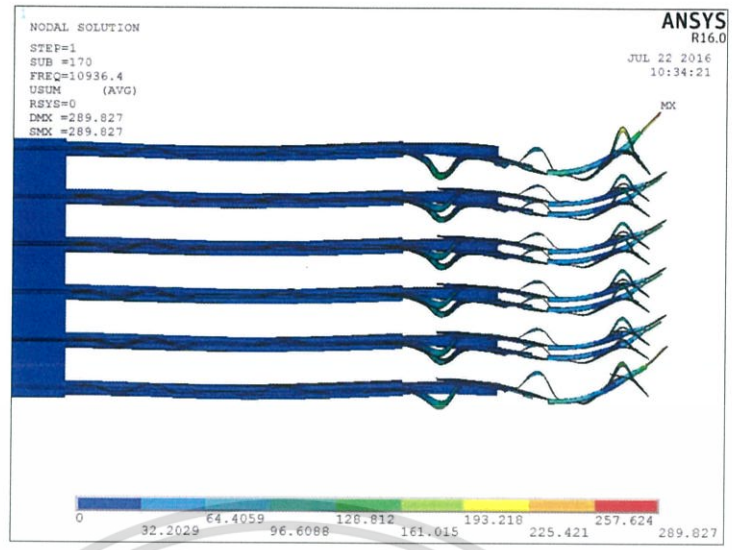

Figure 5.7 Suspension first torsion + FOS second bending, 10936 Hz

Figure 5.7 shows the suspension first torsion and FOS second bending mode. Its associated natural frequency is 10.936 kHz. This mode shows coupling frequency between the arms and the FOS. This mode tends to create this slider positioning error or track-misregistration because the suspensions have been twisted in horizontal direction and also caused by arm torsion behavior.

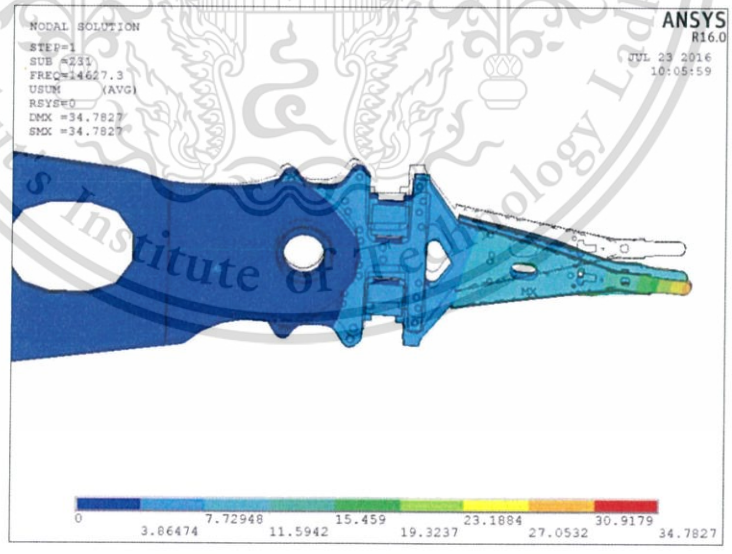

Figure 5.8 Suspension sway, 14870 Hz

Figure 5.8 shows the suspension sway mode. Its associated natural frequency is 14.870 kHz. The suspension sway mode is a horizontal movement. This mode tends to create slider positioning error.

5.2 Harmonic analysis results

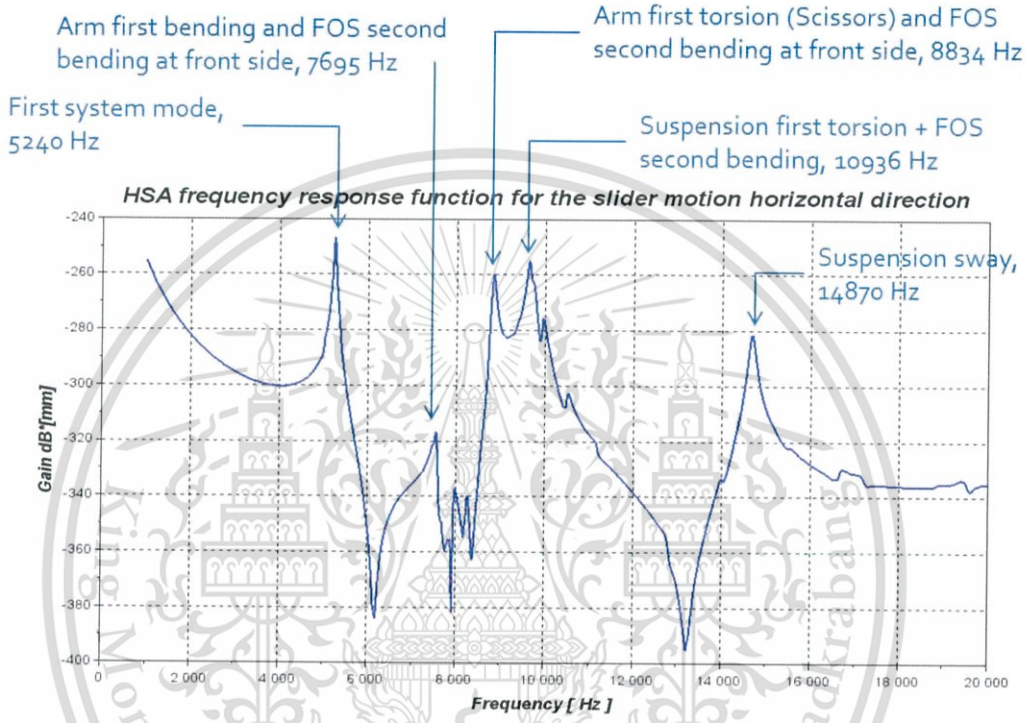

Figure 5.9 HSA frequency response function for the slider motion horizontal direction

Figure 5.9 shows the frequency response of the slider motion in horizontal direction. The vertical axis is a displacement magnitude in dB unit and the horizontal axis is the exciting frequency varied from 0 to 20 kHz. In the experiment, the HSA was excited at VCM coil and LDV measurement was placed on slider in-Y direction. There are many resonance modes that appear in this frequency range.

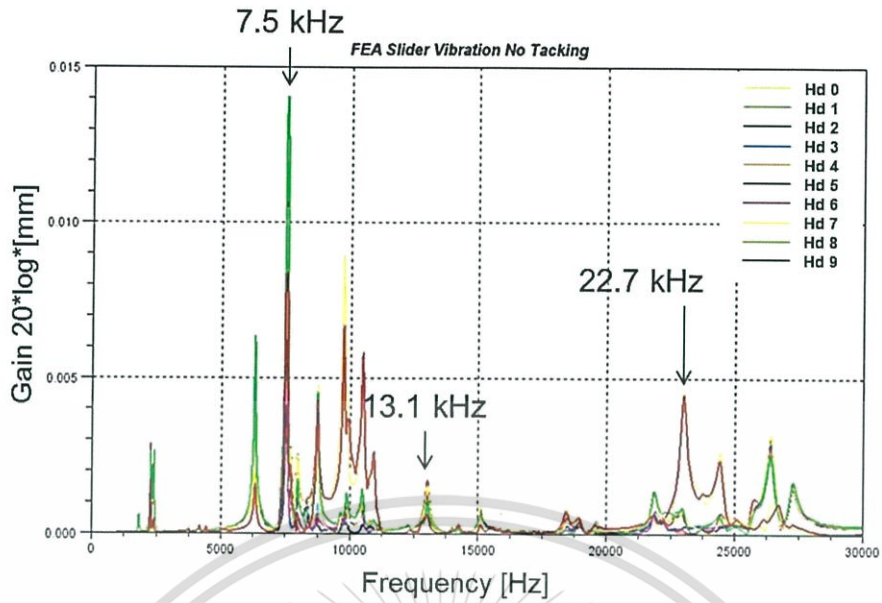

Figure 5.10 HSA windage plot for slider horizontal direction

Figure 5.10 shows the frequency response of the slider motion in horizontal direction. The vertical axis is a displacement magnitude in dB unit and the horizontal axis is the exciting frequency varied from 0 to 30 kHz. In the experiment, the HSA was excited along the FOS and LDV measurement was placed on slider in-Y direction. The forces applied on the FOS was transferred from fluid dynamic result which simulated by ANSYS CFX. The graph dominant frequency at 7.5 kHz, which is the applied force excitation to the slider head.

5.3 Vortex shedding result

5.3.1 Vortex shedding mathematical calculation

Vortex shedding frequency related to HSA FOS resonance depends on upstream velocity, Strouhal number and the object diameter. The vortex shedding phenomenon is describable in the term of a non-dimensional number as shown in Eq. (3.1).

The flow concerned in this study corresponds to a turbulent flow of air around a actuator arm. The thickness of actuator arm (H) is 6.6×10^{-4} m. The mean velocity at the inlet is determined from angular velocity at disk speed 7200 RPM. Disk diameter is 3 inch. Upstream velocity is 25 m/s and it is taken as a reference value. μ is the dynamic viscosity of the air at room temperature 22 $^{\circ}$C is 1.81 kg/m-s). All

velocities are normalized by this value. The Reynolds number based on V and L is determined from Eq. (3.2). Reynolds number for this system is derived from the below calculation.

$$Re = \frac{\rho VL}{\mu} = \frac{\left(1.225\frac{kg}{m^3}\right) \times \left(25\frac{m}{s}\right) \times (6.6 \times 10^{-4}m)}{1.81 \times 10^{-5}kg/(m \times s)}$$

$$Re = 1{,}117$$

Flow over rectangular cylinders depends on the aspect ratio. Strouhal number can be estimated from Figure 5.11 by using Re = 1,117. The line from x-axis is drawn vertically until it intersects with the graph, smooth surface case. From the intersecting point, the horizontal line is drawn to the left and the Strouhal number can be determined from the intersecting point on y-axis. Figure 5.11 displays how to get the Strouhal number and its value is 0.2. The result of vortex shedding frequency at the actuator arm downstream can be calculated using Eq. (3.1), as follow,

$$f_s = \frac{(0.20) \times (25)}{6.6 \times 10^{-4}} = 7{,}575\ Hz$$

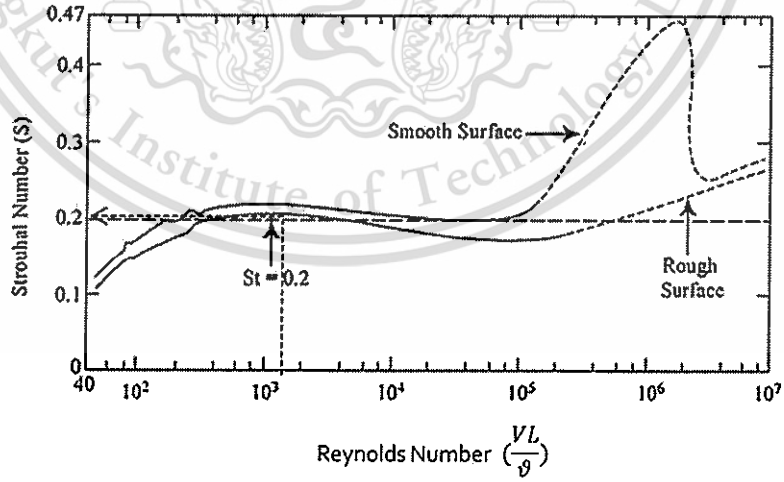

Figure 5.11 Relationship between Strouhal number and Reynolds number for circular cylinders. Data from Liehard (1966). [15]

5.3.2 Vortex shedding frequency simulation using ANSYS Fluent

Figure 5.12 shows the velocity vector and contour plot. The result indicated that the velocity over inner actuator arm is higher than the velocity over outer actuator arm. The velocity vector at actuator arm tailing edge shows unsteady and dynamic internal airflow of the HDD was fluctuated in z-direction and velocity amplitude of inner actuator is higher than outer diameter.

The fluctuation of air velocity at actuator arm tailing edge produces vortex shedding flow and its frequency number can be calculated by getting velocity result in time domain.

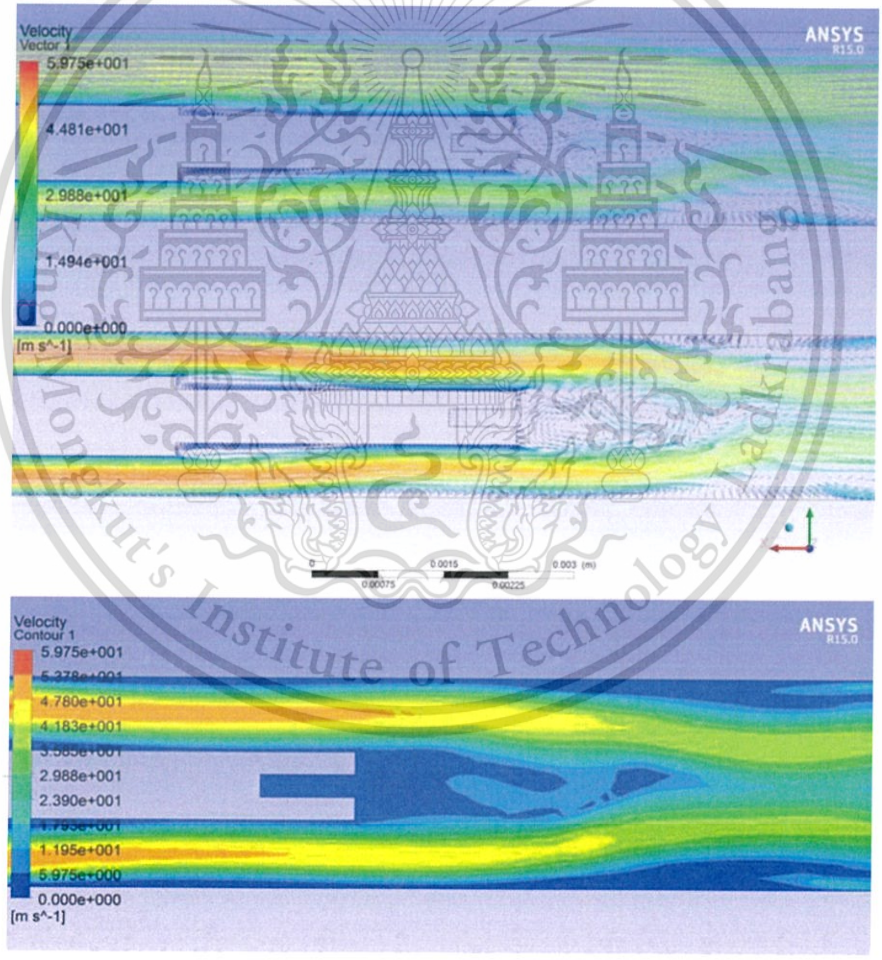

Figure 5.12 Vector and contour plot of air flow

Three points of velocity transient result at actuator arm tailing edge are collected for vortex shedding frequency and velocity amplitude, as shown in Figure 5.13.

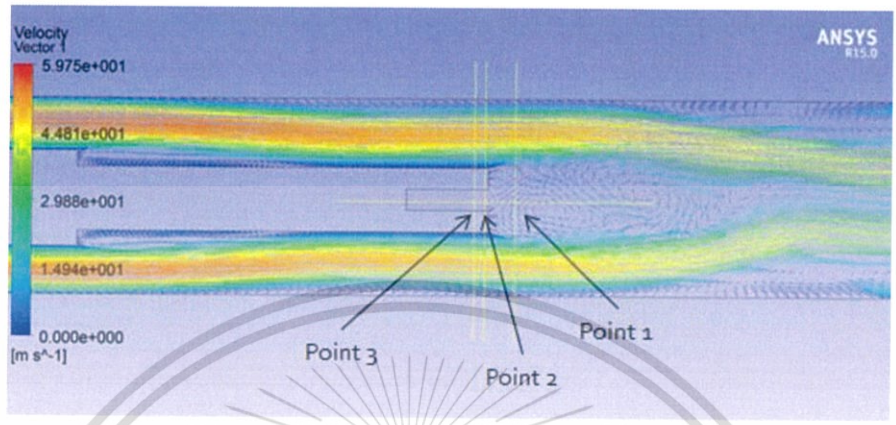

Figure 5.13 Three points of velocity transient result at actuator arm tailing edge

Figure 5.14 shows the velocity magnitude plot of inner actuator arm. As a function of time, it can be observed that the velocity amplitude at different positions of the arm tailing edge is different. Moreover the results show that the magnitudes are harmonically fluctuated.

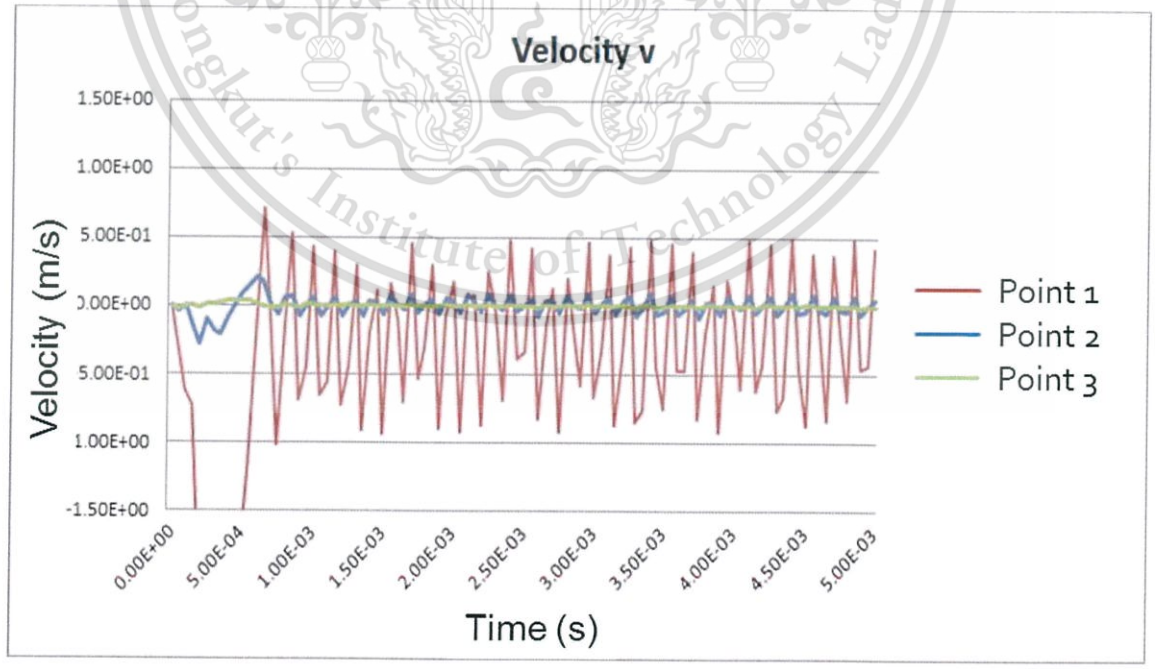

Figure 5.14 Velocity plots of 3 different points

Figure 5.14 shows the velocity magnitude in vertical direction (up-down) at arm tailing edge in time domain. This graph exhibits velocity amplitude of 3 locations at the arm tailing edge, point 1 at outside the arm groove, point 2 at the edge of the arm groove, and point 3 inside the arm groove. This also shows at the outside arm groove produce fluctuation velocity in vertical direction. The velocity start to fluctuate since 0.1 ms, the amplitude fluctuates between -1.0 and 0.75 m/s. At the edge of arm groove, the velocity amplitude is in transition from 0 to 0.1 ms. After that the velocity amplitude in vertical direction is lower than 0.1 m/s. Inside arm groove has not experienced excitation from windage at arm tailing edge so from this simulation graph shown that inside arm groove has a little effect from windage.

The results from finite element analysis show that outside the arm groove had vortex shedding effect with high magnitude around 1 m/s which might generate vibration source to FOS. At the arm edge, very low fluctuation velocity magnitude is observed, and there is no velocity fluctuation inside the arm groove.

In order to identify the exciting frequency, the velocity in time domain, obtained from the finite element result, is transformed to frequency domain by using Fast Fourier Transform (FFT) with no modify input signal filter. The vortex shedding frequency can be determined and its frequency is around 7.1 kHz.

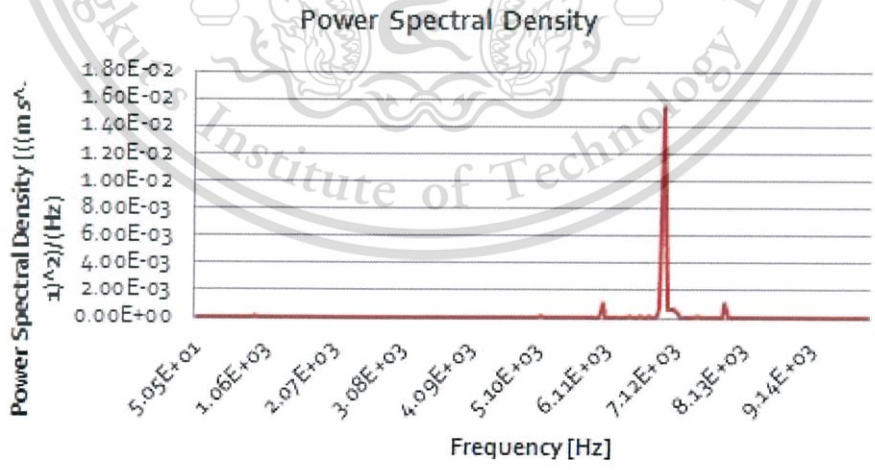

Figure 5.15 Power spectrum of vortex shedding

5.4 Comparison between the FEM and the actual measurement result

5.4.1 FRF comparison

The FEA model validation is necessary to compare with actual measurement using LDV. This comparison will confirm the correctness of the simulation model.

FRF is the frequency response function that applies excitation force at the HSA coil to excite the natural frequency of the HSA system. This thesis will compare only natural frequencies at the main modes that effect to slider vibration. The amplitude will be ignored because of this simulation does not optimize the damping ratio in the input parameters. The maximum discrepancy of natural frequency between actual and FEA is about 19.1% at frequency 13.5 kHz as shown in Table 5.1

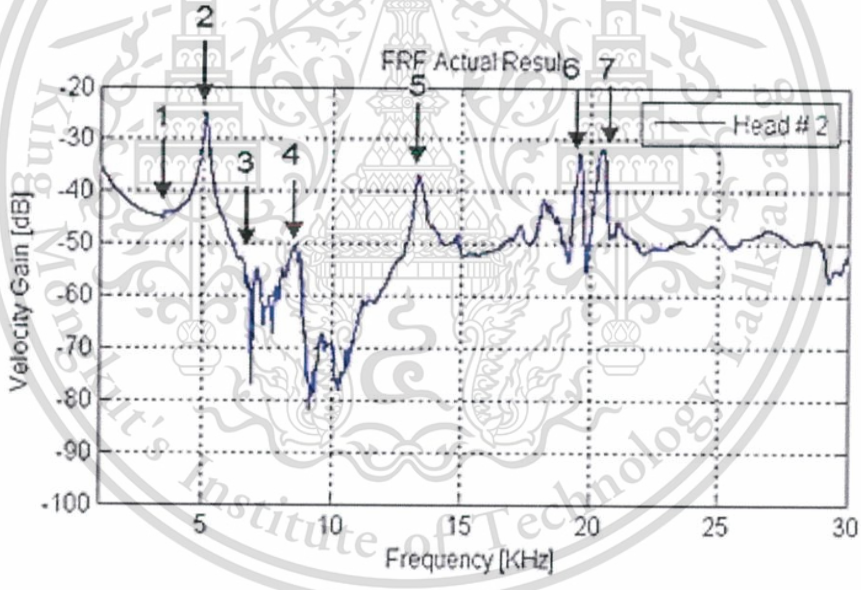

Figure 5.16 Actual FRF measurements of slider head

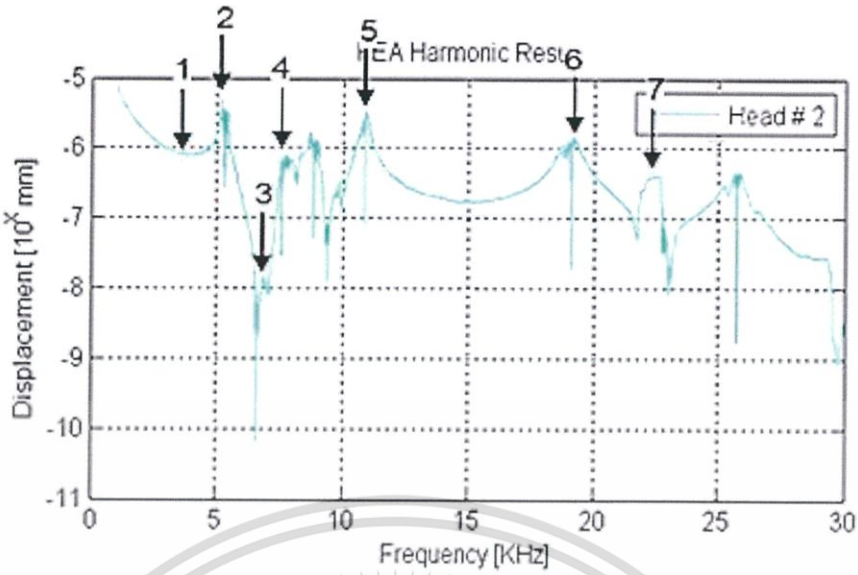

Figure 5.17 Simulation harmonic results of slider head

The identification numbers in Figure 5.16 and Figure 5.17 are resonance frequencies of slider head that had been plot in amplitude versus frequency graph. Those amplitudes will be compared in Table 5.1.

Table 5.1 Natural frequency comparison between actual and FEA results

Mode	Mode name	Frequency (kHz)		% Discrepancy
		Measurement	FEA	
1	Coil torsion	3.5	4.1	17.1%
2	HSA first system	5.2	5.3	1.9%
3	HSA first torsion	6.8	6.3	-7.4%
4	Arm torsion and arm sway	7.6	7.6	0.0%
5	HSA second system	13.5	11	-18.5%
6	HGA sway	18.5	18.7	1.1%
7	HGA third torsion	21	21.7	3.3%

Note* the percent discrepancy is determined by equation as follows,

$$\% \text{ Discrepancy} = \frac{f_{FEA} - f_{actual}}{f_{actual}} \times 100 \qquad (5.1)$$

The comparison between actual and FEA results show good correlation in focusing mode at 7.6 kHz, but some modes did not show good correlation. It might be from model stiffness of some portions and damping ratio parameters. This FEM model will be used to predict resonance frequency and amplitude of the propose methods.

5.4.2 Windage comparison

Windage is the wind excitation model that applied the excitation force from fluid dynamics analysis. This thesis applied force on the FOS only. It will confirm the related frequency between windage force and slider vibration.

From the section 4.2, the mode shape shown that frequency around 7.6 kHz is the slider vibration that is excited by wind excitation.

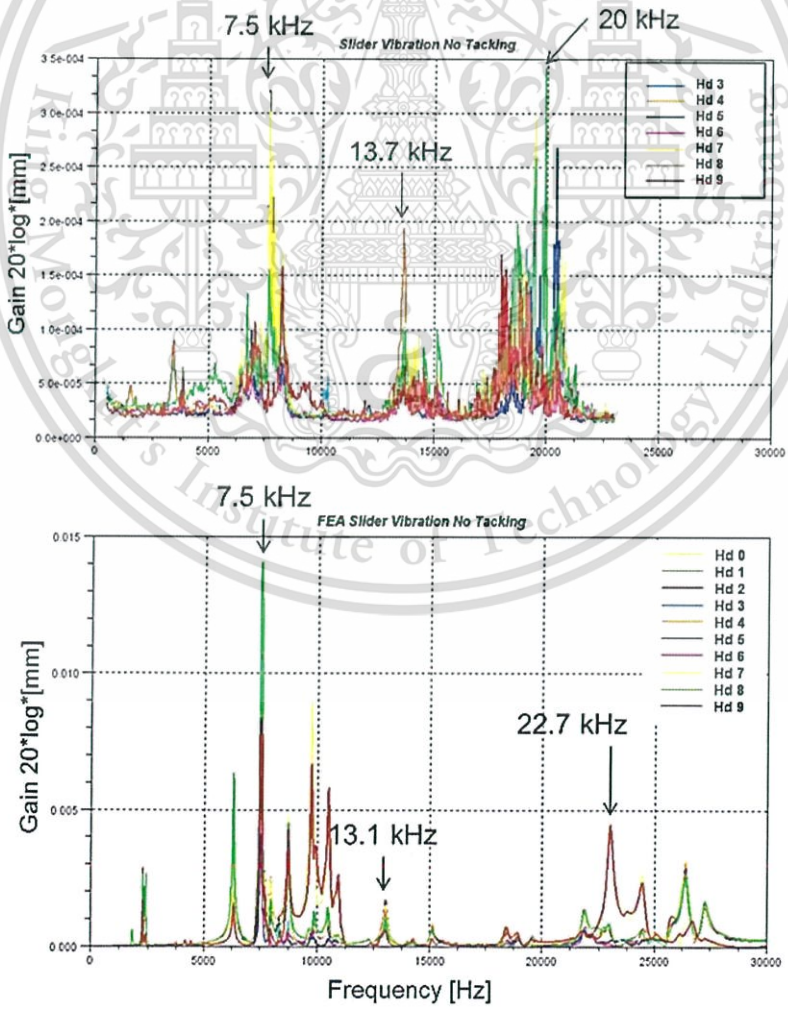

Figure 5.18 Comparison of actual (above) and FEA (below) measurement at slider

Table 5.2 Windage natural frequency comparison between actual and FEA

Mode name	Frequency (kHz)		% Discrepancy
	Actual	FEA	
Arm torsion and arm sway	7.5	7.5	0.0%
HSA second system	13.7	13.1	-4.4%
HGA third torsion	20	22.7	13.5%

Note* the percent discrepancy is determined from Eq. (5.1).

Figure 5.18 is the result of LDV measurement at slider in horizontal direction. This measurement measures while drive is operating and HSA is excited by wind excitation. The LDV actual result shows resonance frequency at 7.5, 13.7 and 20 kHz. Figure 5.18 shows the result from harmonic analysis in which the excitation force from fluid dynamic analysis is applied. The highest amplitude is shown at 7.5 kHz which is expected to be the resonance from wind excitation at the flex of suspension.

This comparison result shows that the applying excitation force at the FOS will excite the slider vibration around 7.5 kHz.

5.5 Comparison of the slider vibration reduction using the proposed methods

This thesis proposes 3 methods to reduce the slider vibration as following,

1. Apply glue to add the damping into the system, namely, Tail tacking.
2. Increase stiffness of the FOS by changing flapper attached location, expect to change the natural frequency of the FOS by putting constrain into the system. Namely, flapper attachment.
3. Reduce force excitation for the windage by re-locating the FOS into the arm slot. Namely, FOS relocation.

The result obtained from each method will be compared with current design. Those results will be measured using single point LDV at slider in horizontal direction.

The data will be collected from windage measurement, amplitude at 7.6 kHz. The results are shown in Table 5.3.

These propose methods will be tested in drive level, None Repeatable Run-Out (NRRO) that is measure recording head position while drive is operating. The result will be shown in column drive % off track in Table 5.3.

Table 5.3 Experimental design and result comparison

Model	HSA	HSA level	Drive	Drive level
	Amplitude	% reduction	% off track	% reduction
Current	2.80×10^{-5}	Baseline	12.55	
Tail tacking	1.70×10^{-5}	-39.3%	8.65	-31.1%
Flapper attachment	2.50×10^{-5}	-10.7%		
FOS relocation	1.80×10^{-5}	-35.7%	8.03	-36.0%

In HSA level, the proposed methods, tail tacking, flapper attachment and FOS relocation can reduce resonance amplitude -39.3%, -10.7% and -35.7%. The tail tacking method had shown the best performance in term of amplitude.

In drive level, flapper attachment was not tested because of HSA level performance is not satisfied. So the proposed methods, tail tacking and FOS relocation can reduce % off track -31.1% and -36.0%. The FOS relocation method showed the best performance in term of drive resonance test.

CHAPTER 6

CONCLUSIONS

6.1 Conclusions

Based on the results obtained from the simulations and the experiments, the conclusions can be drawn as follows,

1) The HSA with FOS vibration characteristics, natural frequencies and mode shapes, were numerically and experimentally investigated. The results obtained from both methods were in good agreement, in term of predicting the mode shapes, but the associated frequencies were different from each other. The maximum discrepancy is about 19.1%.
2) From the harmonic analysis results, it indicates that the main excitation to a slider head vibration is due to vortex shedding on FOS and its exciting frequency is approximately 7.6 kHz.
3) In order to reduce the slider head vibration, the three methods, namely, tail tacking, flapper attachment and FOS relocation, were proposed and their effectiveness on the slider head vibration was experientially studied. The experimental results indicated that the percentage reductions of slider head vibration are 39.3%, 10.7%, and 35.7%, respectively. The tail tacking method yielded highest reduction. However, this method was not actually employed since this method requires the application of adhesive to bond FOS with the actuator arm. In general, the adhesive usage will generate out gassing and leads to particle contamination problem. Thus, practically, the FOS relocation is highly recommended.

6.2 Suggestions for further work

This thesis studied resonance frequency at slider that effected from FOS vibration excitation by windage only 1 position that creates a problem for this product. Actual behavior of HDD, head position is swept on all locations of the disk so another location will create the difference resonance frequency because velocity is different. To predict frequency range effect to slider position need to determine on all location of HDD and fix the problem before ramp up the product.

REFERENCES

[1] Strouhal, V. Ueber eine besondere Art der Tonerregung, Annalen der Physik und Chemie, (1878), 5(10) , 216–251

[2] Nakaguchi, H., Hashimoto, K. and Muto, S. (1968), *An experimental study on aerodynamic drag of rectangular cylinders*, Journal of Japan Aeronautics Space Science, 16(168).

[3] Otsuki Y, Washizu K, Tomizawa H, and Ohya A (1974), *A note on the aeroelastic instability of a prismatic bar with square section*, Journal of Sound and Vibration, 34(2), 233-248.

[4] Okajima, A. (1982), *Strouhal numbers of rectangular cylinders*, Journal of Fluid Mechanics, 123, 379-398

[5] Okajima, A. (1988), *Numerical simulation of flow around rectangular cylinders*, Japanese Journal of Wind Engineering, No. 37, 281-290, October

[6] Tsuda, N., Kubotera, H., Tatewaki, M., Noda, S., Hashiguchi, M. and Maruyama, T., (2003), *Unsteady Analysis and Experimental Verification of the Aerodynamic Vibration Mechanism of HDD Arms*, IEEE Trans. Magn., 39:(2):819-25.

[7] Hirono, Y., Arisaka, T., Nishijima, N., Shimizu, T., Nakamura, S. and Masuda, H., (2004), *Flow-Induced Vibration Reduction in HDD by Using a Spoiler*, IEEE Trans. Magn., 40:(4):3168-70.

[8] E.Y.K. Ng, N.Y. Liu and Y.C.M. Tan, (2011), *Structure Optimization Study of Hard Disk Drives to Reduce Flow-Induced Vibration*

[9] Wikipedia. www.wikipedia.org (https://en.wikipedia.org/wiki/Hard_disk_drive)

[10] Korean Patent Application No. 2003-19139, filed on 27 Mar. 2003, in the Korean Intellectual Property Office

[11] Wikipedia. www.wikipedia.org/Vortex-induced_vibration

[12] Wikipedia. www.wikipedia.org/Vortex_shedding

[13] Wikipedia. www.wikipedia.org/Reynolds_number

[14] www.matweb.com

[15] J. H. Lienhard, Washington State University, (1966), *Locked-in Vortex Shedding Behind Oscillating Circular Cylinders*, with Application to Transmission Lines

[16] ANSYS 16.0

APPENDIX A

PUBLICATION

This work has also been published and presented in International Conference on Engineering Science and Innovative Technology 2016 21-23 April 2016, Phuket, THAILAND

Paper ID 108

The 2nd International Conference on Engineering Science and Innovative Technology (ESIT 2016), Phuket, Thailand, April 21 - 23 2016

Head Stack Assembly Flex Circuit Windage Vibration Reduction

Boripat Naknual[1,*] and Monsak Pimsarn[2]

Abstract

Vibration is a phenomenon that occur frequency in nature. One of the examples is flow induced vibration inside hard disk drive (HDD). The mechanical components inside hard disk drive, especially the actuator system and flex circuit, are very sensitive to flow induced vibration circumstances that cause of recording heads position error. Therefore, this article aims to experimentally and numerically study vibration characteristics of flex circuit of the head stack assembly (HSA) in HDD. The experimental and simulated results confirmed that the main source vibration of flex circuit is from vortex shredding. After that the method of flex circuit vibration reduction is proposed by introducing the spoiler on actuator arm to cover the flex circuit and the measured result shows that the flex circuit is excited with different frequency, due to vortex shredding frequency change, and its vibration amplitude, velocity, reduced by 36 percent.

Keywords : vortex shedding, flow induced vibration, flex circuit, head stack assembly

[1,*] Graduate Student, Department of Data Storage Technology, College of Data Storage Innovation, King Mongkut's Institute of Technology Ladkrabang.

[2] Assistant Professor, Department of Mechanical Engineering, Faculty of Engineering, King Mongkut's Institute of Technology Ladkrabang.

* Corresponding author, E-mail:boripat.naknual@seagate.com

1. Introduction

Windage is the wind excitation while HDD is operating which is main cause of the slider position error. The wind that is generated from disk rotation will excite the HSA components. Flex Circuit is one component of Head Stack Assembly (HSA) which has very thin thickness so it is easy to be excited by wind and generate the vibration effect to slider. To reduce vibration of HSA flex circuit are two main approaches. One is reducing Windage which is vibration generated source and the other is improving Flex circuit stiffness or add constrain. This paper study Windage effect to resonance frequency that relate to recording head position error.

2. Related theory

2.1 Vortex Shedding Frequency

Vortex shedding is an oscillating flow that take place when the air past actuator arm. The air past actuator arm creates low pressure and force on the downstream side of actuator arm. A function of the upstream velocity and the dimension of actuator arm is relate to vortex shedding frequency fs that will excite TGA flex at downstream side. Where U is upstream velocity and D is actuator thickness.

$$f_s = \frac{SU}{D} \qquad (1)$$

Where, fs is the shedding frequency
D is diameter
U inflow speed
S Strouhal number

The Reynolds number is defined as the ratio of momentum forces to viscous forces and consequently quantifies the relative importance of these two types of forces for given flow conditions. Reynolds numbers frequently arise when performing scaling of fluid dynamics problems, and as such can be used to determine dynamic similitude between two different cases of fluid flow. They are also used to characterize different flow regimes within a similar fluid, such as laminar or turbulent flow:

$$Re = \frac{inertial\ forces}{viscous\ forces} = \frac{\rho VL}{\mu} = \frac{VL}{\vartheta} \qquad (2)$$

Where:

V is the maximum velocity of the object relative to the fluid
L is a characteristic linear dimension
μ is the dynamic viscosity of the fluid
ν (nu) is the kinematic viscosity
ρ is the density of the fluid

3. Experiment

3.1 Experiment set-up

The experiments were carried out by Scanning LDV system at Seagate Technology (Thailand) Ltd, set-up is in Figure 1. Hard disk drive spins at 7200 RPM. Actuator arm was located at inner, middle and outer zone of disk. To measure the vibration cause by wind-induce vibration, the test model was set up to measure response frequency range 500 – 15,000 Hz which relate to Head Stack Assembly (HSA). TGA vibration was measured by Laser Doppler Vibrometer (LDV) at resolution line 1600. LDV was set up 125 m/s/V, low pass filter at 100 KHz and high pass filter at 100 Hz.

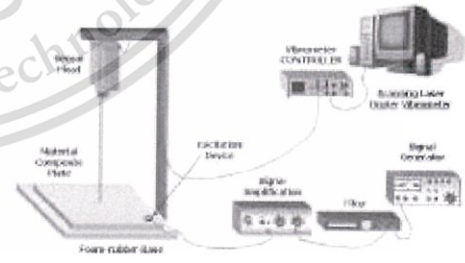

Fig. 1. Schematic of System Setup for Windage Excitation Power Spectrum Test

There are 2 types of resonance measurement in this experiment; one is the LDV measurement at slider to predict recording head miss-position. Another one is Scanning LDV measurement to measure Actuator arm and flex resonance especially.

3.2 Measurement configuration

Outer Diameter (OD) Configuration: Almost of resonance modes appear at FOS rear zone which have no fix constrain between arm groove and TGA.

Middle Diameter (MD) Configuration: The resonance modes appear at same frequency to OD configuration but the amplitude is higher which might be from instructive interference of wind excitation from highest velocity from disk outer diameter. Configurations setting are shown in Fig. 2.

Fig. 2. Left is HSA position at MD configuration. Right is HSA position at OD configuration

4 Results and discussion

4.1 Resonance measurement

Resonant frequency is determined by measure vibrating object motion in time domain and then applies Fast Fourier Transform (FFT) to transform object's motion time domain to frequency domain.

Scanning LDV measurement directly Actuator arm and Flex shown resonance frequency at MD and OD configuration are same frequency range but amplitude at MD configuration is higher than OD configuration. The resonance frequencies of the Actuator arm and Flex are 3.8, 6.1, 7.6 and 8.7 KHz in Fig. 3 (a). LDV measurement at slider found resonance frequency at 7.9 KHz in Fig. 3 (b).

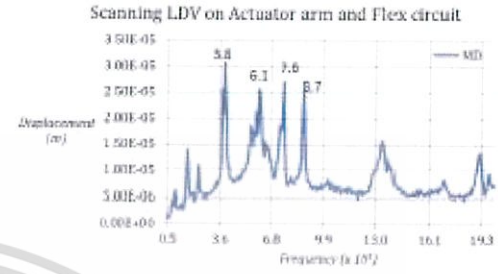

(a)

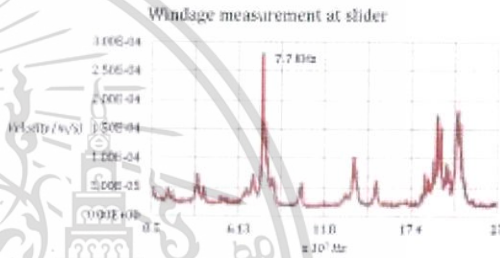

(b)

Fig. 3. (a) Resonance measurement from Scanning LDV at MD configuration. (b) Resonance measurement at slider

4.2 Vibration source model

Vortex shedding frequency relate to HSA flex circuit resonance is depend on upstream velocity, Strouhal number and object diameter, Strouhal (1878) [1] suggested that the regularity of vortex shedding phenomenon is describable in the term of a non-dimensional number;

$$f_s = \frac{SU}{D}$$

The flow concerned in this study corresponds to a turbulent flow of air around a actuator arm. The thickness of actuator arm (H) is 6.6e-4 m. The mean velocity at the inlet is

determined from angular velocity at disk speed 7200 RPM, disk diameter is 3 inch. Upstream velocity is 25 m/s and it is taken as a reference value. μ is the dynamic viscosity of the air at room temperature 22°C is 1.81 kg/(m×s). All velocities are made non-dimensional with this value. The Reynolds number, based on U and H is determined from Eq. (2), Reynolds number for this system is 1,117.

$$Re = \frac{\rho V L}{\mu} = \frac{\left(1.225 \frac{kg}{m^3}\right) \times \left(25 \frac{m}{s}\right) \times (6.6 \times 10^{-4} m)}{1.81 \times 10^{-5} kg/(m \times s)}$$

$$Re = 1{,}117$$

Flow configurations over rectangular cylinders are also strongly dependent of the aspect ratio. Strouhal number can be estimate from figure 4, the Strouhal number is 0.21. Okajima [2] conducted the experiments on the vortex-shedding frequencies and corresponding Strouhal numbers of various rectangular cylinders in a wind tunnel and in a water tank. Reynolds number 1,117. The result vortex shedding frequency at the actuator arm downstream can be calculated by Eq. (1).

$$f_s = \frac{(0.21) \times (25)}{6.6 \times 10^{-4}} = 7{,}954\ Hz$$

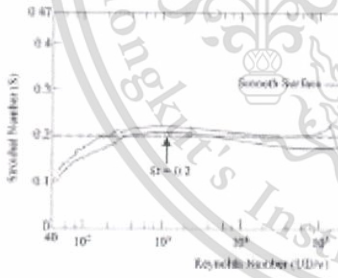

Fig. 4. Relationship between Strouhal number and Reynolds number for circular cylinders. Data from Liehard (1966) and Achembach and Heinecke (1981)

4.3 Numerical modeling

Simulation of fluid dynamic accomplishes through finite element or finite difference schemes. The result shown vortex shedding at the actuator arm downstream that is excitation source of flex circuit of HSA in Fig. 5 (a). Solution propose to reduce vortex shedding effect at the actuator arm downstream that effect to HSA flex circuit. Velocity at actuator arm downstream is reduced in Fig. 5 (b).

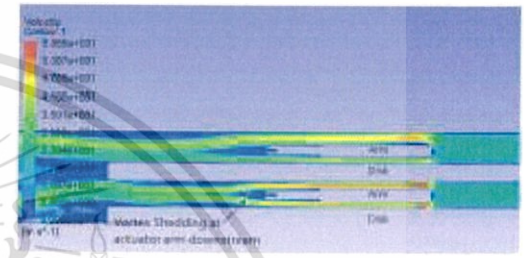

(a)

(b)

Fig. 5. Vector of Vortex shedding at actuator arm downstream

4.4 Actual test result

To reduce vortex shedding frequency at downstream on actuator arm by extend actuator arm to prevent Flex circuit from vortex shedding zone in Fig. 7.

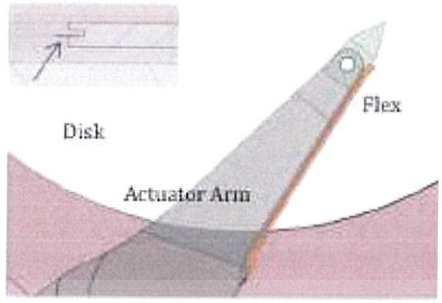

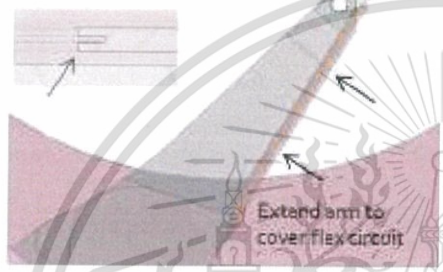

Fig. 6. Actuator arm extended to cover flex circuit to reduce Windage excitation source

Experiment validation is comparing the current HSA without adhesive tacking between flex circuit and arm (No Tacking), current HSA with adhesive tacking 2 dots (Tacking) and extended arm without adhesive tacking (Wider Arm). The actuator arm extended to cover flex circuit can reduce its vibration, measurement at slider shown the vibration at frequency 7.9 KHz is reduced amplitude in Fig. 8 and mode shape of frequency 7.9 KHz is shown in Fig. 9.

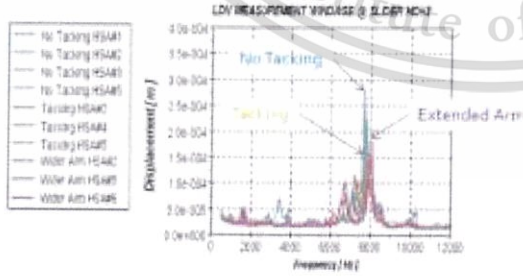

Fig. 8. Windage result measure at slider comparison between 3 designs

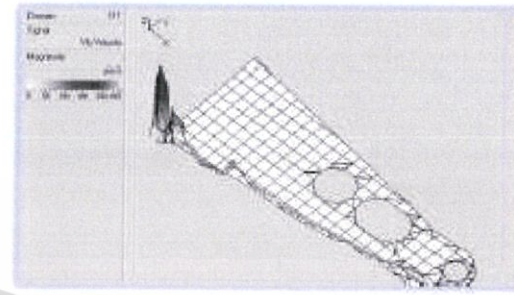

Fig. 9. Mode shape at 7.9 KHz from Scanning LDV

The experiment result shown extended and current arm design with 2 adhesive tacking is similar resonance amplitude while current arm design without adhesive tacking is higher amplitude than the other group in Table 1.

Resonance measurement in drive level is None Repeatable Run-Out (NRRO) that is measure recording head position while drive is operating. The result shown recording head miss-position of current design is 6.08 % of track in Fig. 10 (a) and new design with extended arm to cover HSA flex circuit is 6.22 % of track in Fig. 10 (b).

Table 1 Experiment design and result comparison

Design Name	Arm design	Number of tail tack	Resonance Amplitude (m)
No tacking	Normal	0	2.8×10^{-5}
Tacking	Normal	2	1.7×10^{-5}
Extended Arm		0	1.8×10^{-5}

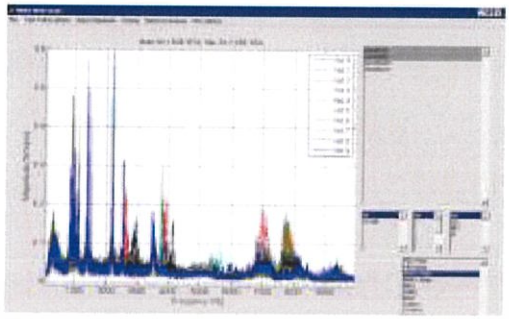

(a)

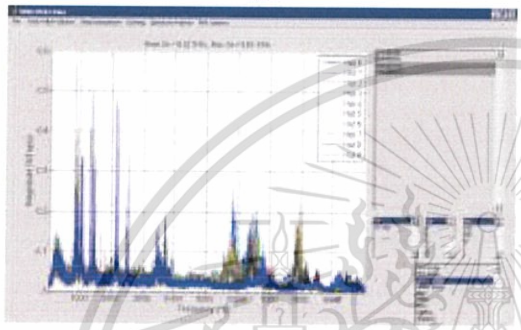

(b)

Fig. 10. Drive resonance measurement None Repeatable Run-Out (NRRO), normal arm with tacking 2 dots (a) and extended arm without tacking (b)

5. Conclusion

This study investigated vibration frequency of flex circuit on HSA that effect to recording head position error, the result shown that slider vibration frequency is related to vortex shedding frequency at actuator arm downstream.

The validate of propose method is to reduce excitation source by extend the actuator arm to cover flex circuit of HSA in HDD, the result shown vibration phenomenal of recording head is reduce by this solution.

6. Reference

[1] Strouhal, V. Ueber eine besondere Art der Tonerregung, Annalen der Physik und Chemie, 1878, 5 (10) (1878), 216–251.

[2] Okajima, A. (1982), "Strouhal numbers of rectangular cylinders", Journal of Fluid Mechanics, 123, 379-398.

[3] Okajima, A. (1988), "Numerical simulation of flow around rectangular cylinders", Japanese Journal of Wind Engineering, No. 37, pp. 281-290, October.

[4] Blevins, (1990) Flow Induced Vibrations, Krieger Publishing Co., Florida.

[5] BLEVINS, R. D. (Ed.) 1990 Flow-induced Vibration. Von Nostrand Reinhold.

[6] Large Eddy Simulation of the flow past a square cylinder, J.S. Ochoa, N. Fueyo

[7] The interaction between flow-induced vibration mechanisms of a square cylinder with varying angles of attack

[8] Determination of the Strouhal Number Based on the Aerodynamic Behavior of Rectangular Cylinders, Chang Koon Choi, Korea

[9] Locked-in Vortex Shedding Behind Oscillating Circular Cylinders, with Application to Transmission Lines, J. H. Lienhard, Washington State University, 1966

APPENDIX B

ELEMENT TYPES

Element Types [16]

SOLID45

SOLID45 is used for the 3-D modeling of solid structures. The element is defined by eight nodes having three degrees of freedom at each node: translations in the nodal x, y, and z directions. The element has plasticity, creep, swelling, stress stiffening, large deflection, and large strain capabilities. A reduced integration option with hourglass control is available.

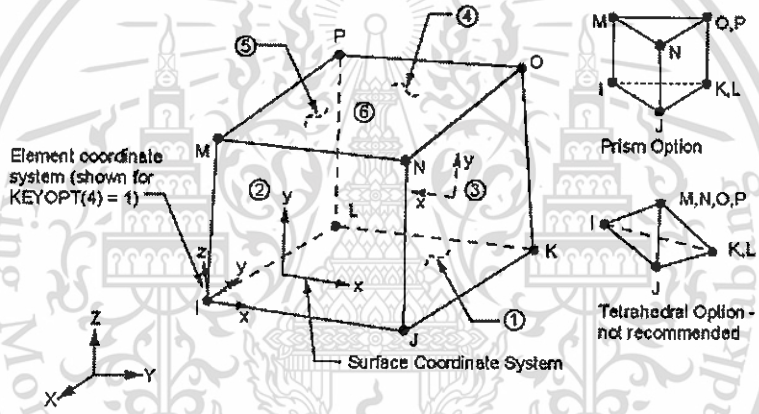

SOLID45 Geometry

Nodes: I, J, K, L, M, N, O, P

Degrees of Freedom: UX, UY, UZ

SHELL43

SHELL41 is a 3-D element having membrane (in-plane) stiffness but no bending (out-of-plane) stiffness. It is intended for shell structures where bending of the elements is of secondary importance. The element has three degrees of freedom at each node: translations in the nodal x, y, and z directions. The element has variable thickness, stress stiffening, large deflection, and a cloth option

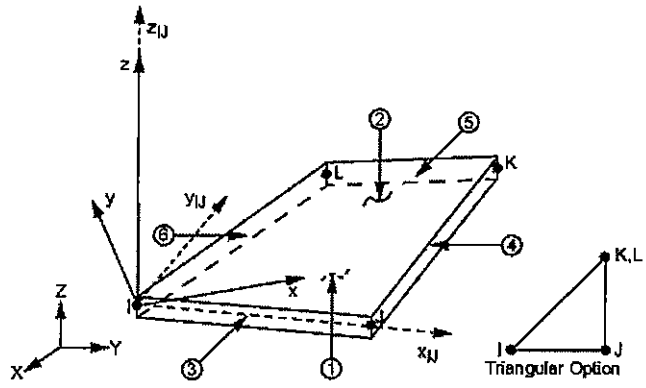

SHELL41 Geometry

Nodes: I, J, K, L

Degrees of Freedom: UX, UY, UZ

SHELL91

COMBIN14 (spring)

COMBIN14 has longitudinal or torsional capability in 1-D, 2-D, or 3-D applications. The longitudinal spring-damper option is a uniaxial tension-compression element with up to three degrees of freedom at each node: translations in the nodal x, y, and z directions. No bending or torsion is considered. The torsional spring-damper option is a purely rotational element with three degrees of freedom at each node: rotations about the nodal x, y, and z axes. No bending or axial loads are considered.

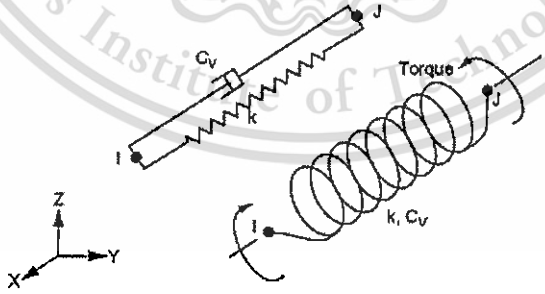

2-D elements must lie in a z = constant plane

COMBIN14 Geometry

Nodes: I, J

Degrees of Freedom: UX, UY, UZ

MASS21

MASS21 is a point element having up to six degrees of freedom: translations in the nodal x, y, and z directions and rotations about the nodal x, y, and z axes. A different mass and rotary inertia may be assigned to each coordinate direction.

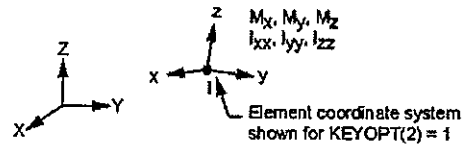

MASS21 Geometry

Nodes: I

Degrees of Freedom: UX, UY, UZ, ROTX, ROTY, ROTZ

PLANE42

PLANE42 is used for 2-D modeling of solid structures. The element can be used either as a plane element (plane stress or plane strain) or as an axisymmetric element. The element is defined by four nodes having two degrees of freedom at each node: translations in the nodal x and y directions. The element has plasticity, creep, swelling, stress stiffening, large deflection, and large strain capabilities. An option is available to suppress the extra displacement shapes.

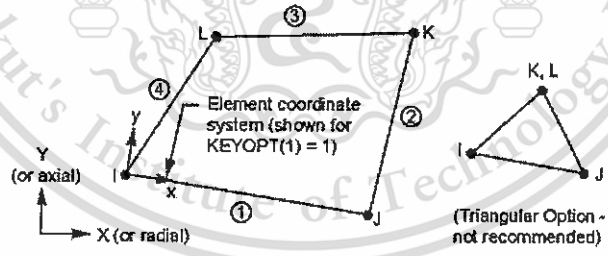

PLANE42 Geometry

Nodes: I, J, K, L

Degrees of Freedom: UX, UY

AUTHOR BIOGRAPHY

Name-Surname:	Mr. Boripat Naknual
Date of Birth:	April 19th, 1981
Present Address:	61/73 Moo 5, Phaholyothin Rd, Klong 1, Klong Luang, Pathum Thani 12120
Education:	2001-2004: Bachelor degree in Aerospace Engineering, Kasetsart University.
Scholarships:	2011-2012 Scholarship for study in Master of Engineering in Data Storage Technology (English program) by NSTDA, KMITL and Seagate Technology (Thailand) Ltd.
Publications:	Boripat N., Monsak P., ***Head Stack Assembly Flex Circuit Windage Vibration Reduction***, International Conference on Engineering Science and Innovative Technology 2016, 21-23 April 2016, Phuket, THAILAND
Experience:	
2010-Present	Seagate Technology (Thailand) Ltd - HSA Process Development
2006-2010	Western Digital (Thailand) Ltd
	- Mechanical Reliability Engineer
	- Advance Manufacturing Engineer